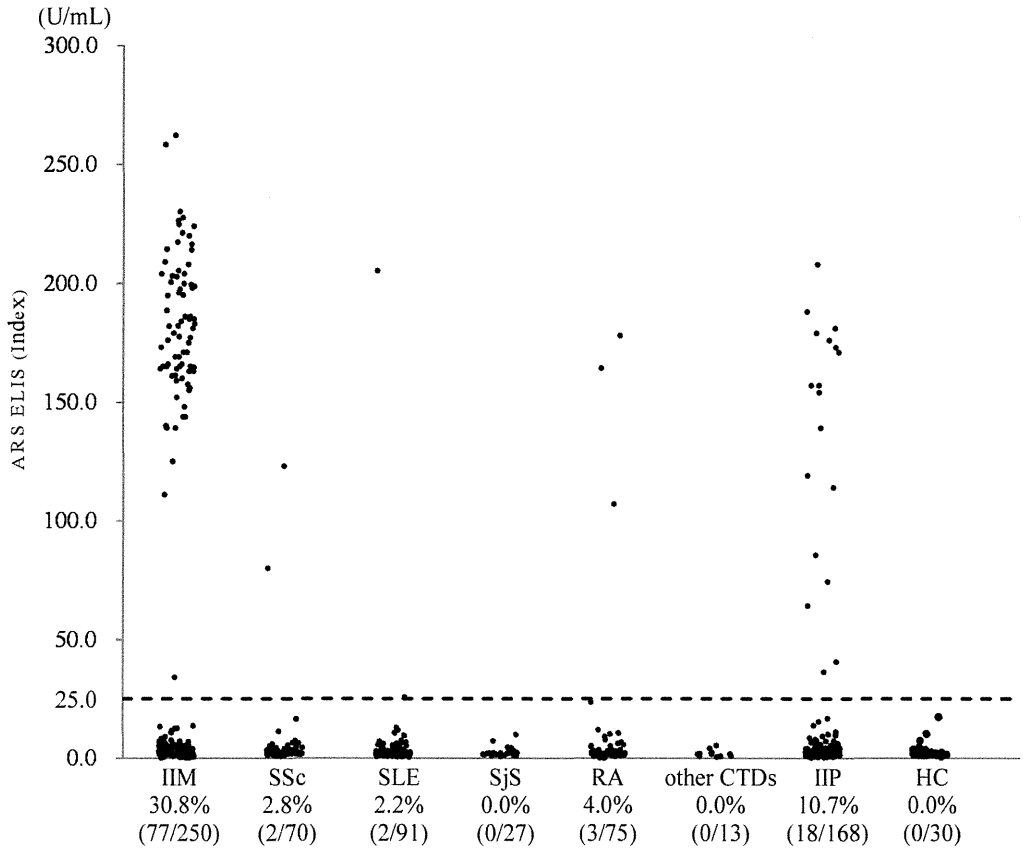

Figure 2. Confirmation of the efficiency of the ELISA system. Using the ELISA system, ARS antibodies were measured in 694 serum samples from patients with various CTDs and IIP, and 30 serum samples from healthy controls. The cutoff value (25 U/mL) is indicated by a horizontal dotted line.
doi:10.1371/journal.pone.0085062.g002

and IP anti-ARS-positive patients showed a better response to initial GC therapy but it can exacerbate the condition more often in anti-ARS-positive than in anti-ARS-negative patients [1,26]. Therefore, anti-ARS antibodies are useful not only in diagnosis, predicting the clinical course and therapy decisions in IIM, but also in classifying IP patients and predicting late-onset myopathy in IP-preceding patients.

An immunoprecipitation assay has been used to detect each anti-ARS antibody but to date, it can only be performed in a limited number of laboratories. To detect them more easily and routinely, we aimed to establish an ELISA system using the six recombinant ARS antigens to simultaneously detect anti-Jo-1, PL-7, PL-12, EJ, OJ, and KS antibodies. We did not include anti-tyrosyl or phenylalanyl synthetase because they have been reported only in one case each. However, some differences in clinical manifestations and prognoses among patients expressing different ARS antibodies, especially between anti-Jo-1 and non-anti-Jo-1 patients, have been observed [14,15]. However, different treatments for patients expressing different anti-ARSs have not been established. Currently, we treat anti-ARS-positive patients

Table 2 The frequency of each anti-ARS antibody in IIM, other CTD and IIP.

		RNA-IP(%)					
	ARS ELISA	**Jo-1**	**PL-7**	**PL-12**	**EJ**	**KS**	**OJ**
IIM	30.8% (77/250)	13.6	13.2	2.0	6.0	0.0	0.8
other CTDs	2.5% (7/276)	0.0	0.0	1.4	0.0	0.7	0.4
IIP	10.7% (18/168)	3.6	2.4	0.6	1.2	2.4	0.0
IPF	5.3% (2/38)	0.0	0.0	2.6	0.0	2.6	0.0
non-IPF	12.3% (16/130)	4.6	3.1	0.0	1.5	2.3	0.0

doi:10.1371/journal.pone.0085062.t002

Table 3 The frequency of each anti-ARS antibody in subsets of IIM.

IIM classification	**Total**	**Jo-1**	**PL-7**	**PL-12**	**EJ**	**KS**	**n (%)**
I polymyositis	107	18	7	3	5	0	33 (30.8)
II dermatomyositis	93	13	10	1	9	0	33 (35.5)
III amyopathic dermatomyositis	23	0	2	0	1	0	3 (13.0)
IV malignancy-associated myositis	7	0	1	0	0	0	1 (14.3)
V juvenile myositis	1	0	0	0	0	0	0 (0)
VI overlap myositis	3	1	0	0	0	0	1 (33.3)
VII unclassified	6	2	3	1	0	0	6(37.5)

doi:10.1371/journal.pone.0085062.t003

Table 4 Comparison of clinical backgrounds between anti-ARS (+) and (−) non-IPF patients.

	non-IPF n = 130		
	anti-ARS		
	(−) n = 114	(+) n = 16	p-value
age at the onset of the disease (yr) mean	69.6±9.5	56.9±14.5	<0.01
female (n; (ratio%))	39(34.2)	12(75.0)	<0.01
chronic (n; (ratio%))	104(91.2)	13(81.3)	N.S
subacute + acute (n; (ratio%))	5(4.4)	1(6.3)	N.S
acute (n; (ratio%))	2(1.8)	1(6.3)	N.S
glucocorticoids(GC) (n;(%))	49(43)	11(68.8)	<0.05
GC + immunosuppressants(IS) (n;(%))	19(16.7)	8(50.0)	<0.01
only drugs other than IS (n;(%))	8(7.0)	2(12.5)	N.S
PaO_2 at rest (Torr) mean	75.9±14.9	86.5±37.4	N.S
SpO_2 at rest (%) mean	95.7±2.4	97.1±2.1	<0.05
SpO_2 after 6 min walk test (Torr) mean	88.6±5.5	86.9±6.0	N.S
%VC (%) mean	87.7±22.5	77.9±17.4	<0.05
%DLCO (%) mean	51.0±19.5	58.0±23.1	N.S
KL-6 (U/mL) mean	1132±949	1287±693	N.S
SP-D (ng/mL) mean	207±180	180±136	N.S

%VC: % vital capacity, %DLCO: % diffusing capacity of carbon monoxide.
doi:10.1371/journal.pone.0085062.t004

with expectation of a standard clinical course in which the disease can recur with tapering of GC and in which exacerbation of IP is associated with a poor prognosis [1,14]. Therefore, presently, we are focusing on determining whether a patient with IIM or IIP is anti-ARS positive or not for the first screening when we begin treatment. This is why we decided to use a mixture of ARS antigens and not just single antigens to detect 'multiple anti-ARS antibodies' simultaneously.

We first prepared recombinant ARSs in *E. coli*, but recombinant PL-7 and OJ did not react well with their corresponding autoantibodies either using immunoblotting or an ELISA. For PL-7, structural conformation was important for antigenic activity because the recombinant PL-7 showed good reactivity only when it was expressed in a eukaryotic Hi-5 cell and was not denatured prior to being measured in the ELISA. Conversely, when recombinant PL-7 was denatured with urea or SDS, it was weakly detected with the PL-7 antibody, although its antigenicity was not completely lost. Such antigenic characteristics have also been reported previously by others [27]. This suggests that the synthetase epitope recognized by the anti-PL-7 antibody is in its native tertiary conformation.

In contrast, recombinant OJ (isoleucyl-tRNA synthetase) was not well detected even when it was expressed in Hi-5 cells and analyzed under non-denaturing conditions. This may be due to the unique feature of this isoleucyl-tRNA synthetase, which is a component of the multi-enzyme complex containing nine ARSs with three nonenzymatic factors [28,29]. In screening tests, positivity of anti-OJ in patients' sera was determined by the pattern of immunoprecipitation using HeLa cell extracts as originally described by Targoff *et al.* [28]. But there is a possibility that some 'anti-OJ antibodies' may recognize other components of the multi-enzyme complex rather than isoleucyl-tRNA synthetase itself, or alternatively the structural conformation of the complex may be important for recognition by anti-OJ, as was previously suggested by Targoff *et al.* [10]. They examined 11 patient sera with anti-OJ for evidence of reaction with other components of the complex. Ten out of 11 sera significantly inhibited enzyme activity of isoleucyl-tRNA synthetase, but some of them also significantly inhibited other ARSs such as leucyl-, lysyl-, or arginyl-tRNA synthetases. Moreover, immunoblot analysis of anti-OJ revealed that the majority of the sera could not identify a shared band and only a few sera recognized isoleucyl-tRNA synthetase. These results suggest that most 'anti-OJ sera' may react with multiple synthetases of the multi-enzyme complex or react with conformational epitopes of the complex. For this reason, we considered that it would be difficult to prepare the immunoreactive OJ antigen as a single molecule; therefore, we developed an ELISA system using the other five recombinant ARSs. This may not significantly affect the sensitivity of the ELISA because the prevalence of anti-OJ antibodies in patients is very low among the six anti-ARS antibodies.

The efficiency of this newly established ELISA system was acceptable because the sensitivity and specificity of the system compared with RNA immunoprecipitation were 97.1% and 99.8%, respectively, even if anti-OJ-positive sera was not excluded. The prevalence of anti-ARS in our IIM cohort was comparable with previous reports [1,2]. It was noteworthy that 10.7% of IIP patients, and in particular, 12.1% of non-IPF patients were positive for anti-ARS antibodies and there were some differences between anti-ARS-positive and negative IIP patients in their clinical backgrounds and treatments. Anti-ARS-positive patients were treated significantly more frequently with GC or the combination of GC and immunosuppressants. However, we are not yet ready to recommend immunosuppressive therapy for anti-ARS-positive IIP patients because we have not yet collected enough data on their clinical response and prognosis. Although some of these anti-ARS-positive IIP patients might develop myopathy later, it suggests that the measurement of anti-ARS antibodies may be useful in stratifying patients into disease subsets, which may help in predicting their clinical course.

A line-blot assay for the detection of multiple MSAs/MAAs (EUROLINE Myositis Profile 3) has been used in which anti-Jo-1, PL-7, PL-12, EJ, and OJ are included. This system can detect and discriminate MSAs/MAAs without further anti-ARS tests, but it does not include anti-KS, which has a stronger association with IIP than myositis [30]. To address this point, our system can more efficiently detect anti-ARS and therefore, is the preferred assay to use for IIP patients than the line-blot assay, although our ELISA does not aim to discriminate specificity for each anti-ARS antibody.

In conclusion, our ELISA system using a mixture of five recombinant ARSs shows similar efficiency to RNA immunoprecipitation and makes it possible to more readily detect anti-ARS antibodies in patients with PM/DM and IIP, and can be widely applied in daily practice.

Supporting Information

Table S1 The list of approval by institutional review boards of all participating centers.
(XLSX)

Acknowledgments

We thank Ms. Tsuboi (Department of Rheumatology and Clinical Immunology, Graduate School of Medicine, Kyoto University) for her excellent assistance with RNA immunoprecipitation assays.

Author Contributions

Conceived and designed the experiments: TM RN. Performed the experiments: TM RN YI YH MS AM KW TH MM MH TT KF KY HK YT NE TS KC HS NT. Analyzed the data: RN YI. Contributed reagents/materials/analysis tools: TM RN YI YH MS AM KW TH MM MH TT KF KY HK YT NE TS KC HS NT. Wrote the paper: RN.

References

1. Yoshifuji H, Fujii T, Kobayashi S, Imura Y, Fujita Y, et al. (2006) Anti-aminoacyl-tRNA synthetase antibodies in clinical course prediction of interstitial lung disease complicated with idiopathic inflammatory myopathies. Autoimmunity 39: 233–241.
2. Mimori T, Imura Y, Nakashima R, Yoshifuji H (2007) Autoantibodies in idiopathic inflammatory myopathy: an update on clinical and pathophysiological significance. Curr Opin Rheumatol 19: 523–529.
3. Nishikai M, Reichlin M (1980) Heterogeneity of precipitating antibodies in polymyositis and dermatomyositis. Characterization of the Jo-1 antibody system. Arthritis Rheum 23: 881–888.
4. Mathews MB, Bernstein RM (1983) Myositis autoantibody inhibits histidyl-tRNA synthetase: a model for autoimmunity. Nature 304: 177–179.
5. Brouwer R, Hengstman GJ, Vree Egberts W, Ehrfeld H, Bozic B, et al. (2001) Autoantibody profiles in the sera of European patients with myositis. Ann Rheum Dis 60: 116–123.
6. Mathews MB, Reichlin M, Hughes GR, Bernstein RM (1984) Anti-threonyl-tRNA synthetase, a second myositis-related autoantibody. Jô Exp Med 160: 420–434.
7. Bunn CC, Bernstein RM, Mathews MB (1986) Autoantibodies against alanyl-tRNA synthetase and tRNAAla coexist and are associated with myositis. Jô Exp Med 163: 1281–1291.
8. Targoff IN, Arnett FC (1990) Clinical manifestations in patients with antibody to PL-12 antigen (alanyl-tRNA synthetase). Amô Jô Med 88: 241–251.
9. Targoff IN, Trieu EP, Plotz PH, Miller FW (1992) Antibodies to glycyl-transfer RNA synthetase in patients with myositis and interstitial lung disease. Arthritis Rheum 35: 821–830.
10. Targoff IN, Trieu EP, Miller FW (1993) Reaction of anti-OJ autoantibodies with components of the multi-enzyme complex of aminoacyl-tRNA synthetases in addition to isoleucyl-tRNA synthetase. Jô Clin Invest 91: 2556–2564.
11. Hirakata M, Suwa A, Nagai S, Kron MA, Trieu EP, et al. (1999) Anti-KS: identification of autoantibodies to asparaginyl-transfer RNA synthetase associated with interstitial lung disease. Jô Immunol 162: 2315–2320.
12. Hashish L TE, Sadanandan P, Targoff IN (2005) Igentification of autoantibodies to tyrosyl-tRNA synthetase in dermatomyositis with features consistent with antisynthetase syndrome [abstract]. Arthritis Rheum 52: S312.
13. Betteridge Z, Gunawardena H, North J, Slinn J, McHugh N (2007) Anti-synthetase syndrome: a new autoantibody to phenylalanyl transfer RNA synthetase (anti-Zo) associated with polymyositis and interstitial pneumonia. Rheumatology (Oxford) 46: 1005–1008.
14. Aggarwal R, Cassidy E, Fertig N, Koontz DC, Lucas M, et al. (2013) Patients with non-Jo-1 anti-tRNA-synthetase autoantibodies have worse survival than Jo-1 positive patients. Ann Rheum Dis.
15. Hervier B, Devilliers H, Stanciu R, Meyer A, Uzunhan Y, et al. (2012) Hierarchical cluster and survival analyses of antisynthetase syndrome: phenotype and outcome are correlated with anti-tRNA synthetase antibody specificity. Autoimmun Rev 12: 210–217.
16. Bohan A, Peter JB (1975) Polymyositis and dermatomyositis (first of two parts). Nô Englô Jô Med 292: 344–347.
17. (1980) Preliminary criteria for the classification of systemic sclerosis (scleroderma). Subcommittee for scleroderma criteria of the American Rheumatism Association Diagnostic and Therapeutic Criteria Committee. Arthritis Rheum 23: 581–590.
18. Arnett FC, Edworthy SM, Bloch DA, McShane DJ, Fries JF, et al. (1988) The American Rheumatism Association 1987 revised criteria for the classification of rheumatoid arthritis. Arthritis Rheum 31: 315–324.
19. Tan EM, Cohen AS, Fries JF, Masi AT, McShane DJ, et al. (1982) The 1982 revised criteria for the classification of systemic lupus erythematosus. Arthritis Rheum 25: 1271–1277.
20. Watanabe K, Handa T, Tanizawa K, Hosono Y, Taguchi Y, et al. (2011) Detection of antisynthetase syndrome in patients with idiopathic interstitial pneumonias. Respir Med 105: 1238–1247.
21. Sato T, Fujii T, Yokoyama T, Fujita Y, Imura Y, et al. (2010) Anti-U1 RNP antibodies in cerebrospinal fluid are associated with central neuropsychiatric manifestations in systemic lupus erythematosus and mixed connective tissue disease. Arthritis Rheum 62: 3730–3740.
22. Towbin H, Staehelin T, Gordon J (1979) Electrophoretic transfer of proteins from polyacrylamide gels to nitrocellulose sheets: procedure and some applications. Proc Natl Acad Sciô Uô Sô A 76: 4350–4354.
23. Ghirardello A, Zampieri S, Tarricone E, Iaccarino L, Bendo R, et al. (2006) Clinical implications of autoantibody screening in patients with autoimmune myositis. Autoimmunity 39: 217–221.
24. Matsushita T, Hasegawa M, Fujimoto M, Hamaguchi Y, Komura K, et al. (2007) Clinical evaluation of anti-aminoacyl tRNA synthetase antibodies in Japanese patients with dermatomyositis. Jô Rheumatol 34: 1012–1018.
25. Friedman AW, Targoff IN, Arnett FC (1996) Interstitial lung disease with autoantibodies against aminoacyl-tRNA synthetases in the absence of clinically apparent myositis. Semin Arthritis Rheum 26: 459–467.
26. Love LA, Leff RL, Fraser DD, Targoff IN, Dalakas M, et al. (1991) A new approach to the classification of idiopathic inflammatory myopathy: myositis-specific autoantibodies define useful homogeneous patient groups. Medicine (Baltimore) 70: 360–374.
27. Dang CV, Tan EM, Traugh JA (1988) Myositis autoantibody reactivity and catalytic function of threonyl-tRNA synthetase. FASEBô J 2: 2376–2379.
28. Targoff IN (1990) Autoantibodies to aminoacyl-transfer RNA synthetases for isoleucine and glycine. Two additional synthetases are antigenic in myositis. Jô Immunol 144: 1737–1743.
29. Quevillon S, Robinson JC, Berthonneau E, Siatecka M, Mirande M (1999) Macromolecular assemblage of aminoacyl-tRNA synthetases: identification of protein-protein interactions and characterization of a core protein. Jô Mol Biol 285: 183–195.
30. Hirakata M, Suwa A, Takada T, Sato S, Nagai S, et al. (2007) Clinical and immunogenetic features of patients with autoantibodies to asparaginyl-transfer RNA synthetase. Arthritis Rheum 56: 1295–1303.

PLOS ONE

Severity and Patterns of Blood-Nerve Barrier Breakdown in Patients with Chronic Inflammatory Demyelinating Polyradiculoneuropathy: Correlations with Clinical Subtypes

Fumitaka Shimizu[1], Setsu Sawai[2], Yasuteru Sano[1], Minako Beppu[2], Sonoko Misawa[2], Hideaki Nishihara[1], Michiaki Koga[1], Satoshi Kuwabara[2], Takashi Kanda[1]*

1 Department of Neurology and Clinical Neuroscience, Yamaguchi University Graduate School of Medicine, Ube, Japan, **2** Department of Neurology, Graduate School of Medicine, Chiba University, Chiba, Japan

Abstract

Objective: Chronic inflammatory demyelinating polyradiculoneuropathy (CIDP) is currently classified into clinical subtypes, including typical and atypical forms (multifocal acquired demyelinating sensory and motor neuropathy (MADSAM) and distal acquired demyelinating symmetric neuropathy (DADS)). The aim of this study was to elucidate the patterns and severity of breakdown of the blood-nerve barrier (BNB) in each CIDP subtype.

Methods: We evaluated the effects of sera obtained from patients with typical CIDP, MADSAM and DADS and control subjects on the expression levels of tight junction proteins and transendothelial electrical resistance (TEER) value in human peripheral nerve microvascular endothelial cells (PnMECs).

Results: The sera obtained from the patients with the three clinical phenotypes of CIDP decreased the amount of claudin-5 protein levels and TEER values in the PnMECs. In addition, the sera obtained from typical CIDP patients more prominently reduced claudin-5 protein levels and TEER values in the PnMECs than did that obtained from the MADSAM and DADS patients. Furthermore, the severity of BNB disruption after exposure to the sera was associated with higher Hughes grade, lower MRC score, more pronounced slowing of motor nerve conduction in the median nerve and higher frequency of abnormal temporal dispersion.

Conclusions: Sera derived from typical CIDP patients destroy the BNB more severely than those from MADSAM or DADS patients. The extent of BNB disruption in the setting of CIDP is associated with clinical disability and demyelination in the nerve trunk. These observations may explain the phenotypical differences between CIDP subtypes.

Citation: Shimizu F, Sawai S, Sano Y, Beppu M, Misawa S, et al. (2014) Severity and Patterns of Blood-Nerve Barrier Breakdown in Patients with Chronic Inflammatory Demyelinating Polyradiculoneuropathy: Correlations with Clinical Subtypes. PLoS ONE 9(8): e104205. doi:10.1371/journal.pone.0104205

Editor: Mária A. Deli, Hungarian Academy of Sciences, Hungary

Received May 12, 2014; **Accepted** July 6, 2014; **Published** August 8, 2014

Data Availability: The authors confirm that all data underlying the findings are fully available without restriction. All relevant data are within the paper and its Supporting Information files.

Funding: This work was supported in part by research grants (Nos. 24790886, Nos. 22790821, and Nos. 23659457) from the Japan Society for the Promotion of Science, Tokyo, Japan, by research grant (K2002528) from Health and Labor Sciences Research Grants for research on intractable diseases (Neuroimmunological Disease Research Committee) from the Ministry of Health, Labor and Welfare of Japan, by Intramural Research Grant (25–4) for Neurological and Psychiatrical Disorders of National Center of Neurology and Psychiatry and also by the Translational Research Promotion Grant from Yamaguchi University Hospital. The funders had no role in study design, data collection and analysis, decision to publish, or preparation of the manuscript.

Competing Interests: The authors declare that there is no duality of interest associated with this manuscript.

* Email: tkanda@yamaguchi-u.ac.jp

Introduction

Chronic inflammatory demyelinating polyradiculoneuropathy (CIDP) is a rare autoimmune-mediated neuropathy thought to constitute a group of heterogeneous disorders involving a wide range of clinical phenotypes, variable clinical course and differing responses to immunotherapy [1,2]. The Joint Task Force of the European Federation of Neurological Societies and Peripheral Nerve Society (EFNS/PNS) convened in 2010 divided CIDP into two clinical subtypes: "typical CIDP (t-CIDP)," the classical pattern of CIDP, and "atypical CIDP," which include multifocal acquired demyelinating sensory and motor neuropathy (MADSAM) and distal acquired demyelinating symmetric neuropathy (DADS) [3]. t-CIDP is clinically defined by the presence of chronically progressive or recurrent symmetrical proximal and distal weakness and sensory dysfunction in all extremities developing over at least two months and likely affects a relatively uniform group of patients [4,5]. In contrast, MADSAM neuropathy is characterized by an asymmetrical multifocal pattern of motor and sensory impairment (mononeuropathy multiplex) likely representing an asymmetrical variant of CIDP [6,7]. On the other hand, DADS neuropathy is characterized by symmetrical sensory

and motor polyneuropathy of the distal upper and lower limbs predominantly associated with muscle weakness and/or sensory disturbances in the distal limbs [8,9]. These three CIDP subtypes share a common feature, namely, chronic demyelinative neuropathy of supposed immune origin; however, the different clinical phenotypes appear to result from differences in the underlying immunopathogenesis [10].

Various previous reports have demonstrated that the pathological breakdown of the blood-nerve barrier (BNB), which allows for the entry of immunoglobulins, cytokines and chemokines into the peripheral nerve system (PNS) parenchyma, is a key event in the disease process of CIDP [11,12,13], and the result of electrophysiological examinations have led to a new hypothesis concerning the pathogenesis of CIDP, namely that differences in the degree of BNB malfunction partly determine the differences in both the distribution of demyelinative lesions and clinical phenotypes observed between t-CIDP and MADSAM neuropathy [10,14,15]. In the present study, we evaluated the contributions of humoral factors in sera obtained from patients with each clinical subtype of CIDP to BNB breakdown and clarified the association between BNB disruption and clinical profiles using our previously established human BNB-derived immortalized endothelial cells [16].

Materials and methods

Serum and cerebrospinal fluid samples

The study protocol was approved by the ethics committee of Yamaguchi University and Chiba University. All patients consented to participate and written informed consent was obtained from each subject. Serum was collected from a total of 25 CIDP patients with t-CIDP (n = 12), MADSAM (n = 10) and DADS (n = 3) in the initial progressive phase of the disease or at relapse, without either corticosteroid or intravenous immunoglobulin (IVIg) treatment, diagnosed at Chiba University Hospital or Yamaguchi University Hospital. All patients fulfilled the diagnostic criteria for CIDP based on the guidelines reported by the EFNS/PNS 2010 [3]. The inclusion criteria was a diagnosis of definitive or probable CIDP. None of the patients with DADS had anti-myelin-associated glycoprotein (MAG) antibodies. Sera obtained from 10 healthy individuals served as normal controls. All serum samples were inactivated at 56°C for 30 minutes just prior to use. Cerebrospinal fluid (CSF) samples obtained from the 25 patients with CIDP were analyzed with respect to the protein level in the CSF, the IgG index and/or CSF/serum albumin ratio (Q Alb). The clinical and electrophysiological data for all CIDP patients were analyzed. The clinical parameters included the Hughes functional grading scale [17], which was used as a functional assessment, and the total Medical Research Council (MRC) scale for four muscle groups (deltoid, wrist extensor, iliopsoas and tibialis anterior muscles). All 25 patients received immune system-modulating treatment, including corticosteroids and IVIg. Treatment was considered to be effective if the patient's condition, including the Hughes scale and MRC score, was found to have improved after therapy. Nerve conduction studies were performed according to conventional procedures and using standard electromyography machine (Neuropack M1, Nihon Kohden, Tokyo, Japan; Viking 4, Nicolet Biomedical Japan, Tokyo, Japan). Motor nerve studies of the median, ulnar and tibial nerves were performed, including F wave analyses. The terminal latency index (TLI) was calculated based on the following formula: TLI = terminal distance (mm)/(distal latency (ms) × conduction velocity (m/s)). A partial motor conduction block was defined as a more than a 50% reduction in the compound muscle action potentials (CMAP) between the stimulus sites, and abnormal temporal dispersion was defined as a more than 30% increase in duration between the proximal and distal CMAP, in accordance with the EFNS/PNS guidelines [3].

Cell culture and treatment

Immortalized human peripheral nerve microvascular endothelial cells (PnMECs), termed "FH-BNBs", were generated previously in our laboratory [16]. The cells were cultured in medium [Dulbecco's modified Eagle's medium (DMEM; Sigma, St. Louis, MO, USA) containing 10% fetal bovine serum (FBS; Sigma, St. Louis, MO, U.S.A) and antibiotics] with 10% patient serum or culture medium containing 10% FBS, which was used as a control, in an incubator at 37°C with 5% CO_2/air. The cells were maintained for either 24 hours to measure the transendothelial electrical resistance (TEER) value or 48 hours to extract total proteins.

Reagents

We purchased polyclonal anti-claudin-5 and anti-occludin antibodies from Zymed (San Francisco, CA, U.S.A). Polyclonal anti-actin antibodies were purchased from Santa Cruz (Santa Cruz, CA, U.S.A).

Western blot analysis

After boiling, aliquots containing equal amounts of protein (15 μg) were separated via SDS-PAGE (Bio-Rad, Hercules, CA). The proteins were then transferred onto nitrocellulose membranes (Amersham, Chalfont, UK), as previously described [18]. The membranes were subsequently treated with the relevant primary antibodies (dilution: 1:100) for two hours and then incubated with the secondary antibodies (dilution: 1:2,000) for one hour at room temperature. Finally, the proteins were visualized using an enhanced chemiluminescence detection system (ECL-prime, Amersham, UK). The optical density of each band was assessed using the Quantity One software program (Bio-Rad).

Transendothelial electrical resistance (TEER) studies

The TEER values in the cell layers were measured using a Millicell electrical resistance apparatus (Endohm-6 and EVOM, World Precision Instruments, Sarasota, FL, U.S.A), according to the manufacturer's instructions. The cells were seeded (1×10^6 cells/insert) on collagen-coated Transwell inserts (pore size: 0.4 μm, effective growth area: 0.3 cm^2, BD Bioscience, Sparks, MD, USA), and the TEER value for each insert was calculated following treatment with each type of medium (non-conditioned medium was used as a control, the conditioned medium contained 10% patient serum) for 24 hours by subtracting the blank from each reading. Each condition was tested in triplicate for each experiment.

Data analysis

Differences in the median values between the groups were examined according to the Mann-Whitney U test, with two-sided P value of <0.05 considered to be statistically significant. Pearson correlation coefficients were used to test the associations. All statistical analyses were performed using the IBM SPSS statistical software program, version 21J.

Results

Clinical characteristics

The clinical profiles of patients with t-CIDP, MADSAM and DADS are summarized in Table 1. The mean Hughes grade was

significantly higher in the t-CIDP patients than in the MADSAM or DADS patients and in the MADSAM patients than in the DADS patients. In addition, significantly lower mean MRC values for both the total score for the four muscle groups and the iliopsoas alone were observed in the t-CIDP patients compared to those noted in the MADSAM and DADS patients. Meanwhile, the mean CSF protein concentration was higher in the t-CIDP and DADS patients than in the MADSAM patients. Based on the results of the electrophysiological examinations of the median nerve, the t-CIDP and DADS patients demonstrated a more prolonged average motor nerve distal latency than the MADSAM patients, and while the t-CIDP patients displayed greater slowing of mean motor nerve conduction than the MADSAM patients. Furthermore, a higher frequency of conduction block was observed in the MADSAM patients than in the t-CIDP patients. In contrast, the MADSAM patients exhibited temporal dispersion much less frequently than did the t-CIDP and DADS patients.

The sera obtained from the patients with t-CIDP, MADSAM and DADS disrupted the BNB

We first examined the effects of the sera obtained from the patients with the three clinical subtypes of CIDP on the expression levels of tight junction proteins and the TEER values in the FH-BNBs. Consequently, the protein ratio of claudin-5 to actin proteins was significantly lower in the FH-BNBs exposed to sera from the patients with t-CIDP, MADSAM and DADS than in those incubated with sera from the healthy controls, as determined in a Western blot analysis (**Figs. 1 A–E**). In contrast, the ratio of occludin to actin proteins in the FH-BNBs did not change after a challenge with the sera obtained from the CIDP patients or healthy controls (**Figs. 1A–D, F**). Meanwhile, the TEER values in the FH-BNBs were significantly decreased following exposure to the sera obtained from the t-CIDP, MADSAM and DADS patients in comparison to that observed after exposure to sera of the healthy control (**Fig. 1G**). Furthermore, the ratio of claudin-5 to actin proteins and the TEER values observed after exposure to the sera obtained from t-CIDP patients were significantly lower than those observed after exposure to the sera obtained from the MADSAM and DADS patients (**Figs. 1E, G**). Moreover, the TEER values observed after exposure to the sera obtained from the DADS patients were significantly lower than those observed after exposure to the sera obtained from the MADSAM patients, although the ratio of claudin-5 to actin proteins was not significantly different between the two groups (**Figs. 1E, G**).

Correlations between the clinical, laboratory and electrophysiological findings and BNB malfunction in the patients with CIDP

We next examined the associations between the clinical, laboratory and electrophysiological findings and the ratio of claudin-5 to actin proteins and/or the TEER values in the FH-BNBs exposed to the sera from the CIDP patients. Consequently, the decrease in either the claudin-5 protein level or TEER value in the FH-BNBs was found to be associated with the clinical severity.

Table 1.

	t-CIDP (n = 12)	MADSAM (n = 10)	DADS (n = 3)	
	Mean (±SD), Percent [number]	Mean (±SD), Percent [number]	Mean (±SD), Percent [number]	p Value
Clinical profile				
Age (year)	56 (±12)	56 (±12)	53 (±6)	NS
Male: Female	9:3	8:2	2:1	NS
Disease duration (year)	5.2 (±6.9)	5.4 (±5.4)	3.2 (±1)	NS
Hughes grade scale	2.83 (±0.94)	1.7 (±1.06)	1 (±0)	0.011*, 0.007**, 0.037***
Response to treatment	67% [8/12]	80% [8/10]	100% [3/3]	NS
MRC score				
Total (deltoid+ wrist extensor + iliopsoas + tibialis anterior)	15.7 (±2.6)	18.3 (±1.5)	19.7 (±0.6)	0.015*, 0.013**
CSF protein (mg/dl)	95.3 (±34.7)	55.8 (±31.4)	114.9 (±63.7)	0.002*, 0.028***
CSF IgG index	0.610 (±0.099)	0.560 (±0.134)	0.573 (±0.016)	NS
CSF Q Albumin	0.028 (±0.047)	0.009 (±0.006)	0.014 (±0.011)	NS
Motor conduction study				
Median nerve				
Distal latency (ms)	9.0 (±5.9)	4.7 (±1.0)	14.3 (±12.7)	0.016*, 0.012***
Conduction velocity (m/s)	30.2 (±12.6)	42.3 (±8.3)	41.3 (±0.3)	0.033*
CMAP (mV)	4.6 (±3.4)	6.1 (±3.5)	5.3 (±3.5)	NS
Terminal latency index	0.34 (±0.13)	0.39 (±0.18)	0.18 (±0.11)	NS
Conduction block	58% [7/12]	100% [10/10]	67% [2/3]	0.020*
Temporal dispersion	80% [8/10]	30% [3/10]	100% [3/3]	0.018*, 0.017***

*t-CIDP vs MADSAM, **t-CIDP vs DADS, ***MADSAM vs DADS.
Data are expressed as mean (±SD), median [range] or percent {number}.
t-CIDP, typical chronic inflammatory demyelinating polyradiculoneuropathy; MADSAM, multifocal acquired demyelinating sensory and motor neuropathy; DADS, distal acquired demyelinating symmetric neuropathy, IVIg: Intravenous immunoglobulin, MRC: Medical Research Council, CSF: cerebrospinal fluid, CMAP: compound muscle action potential.
doi:10.1371/journal.pone.0104205.t001

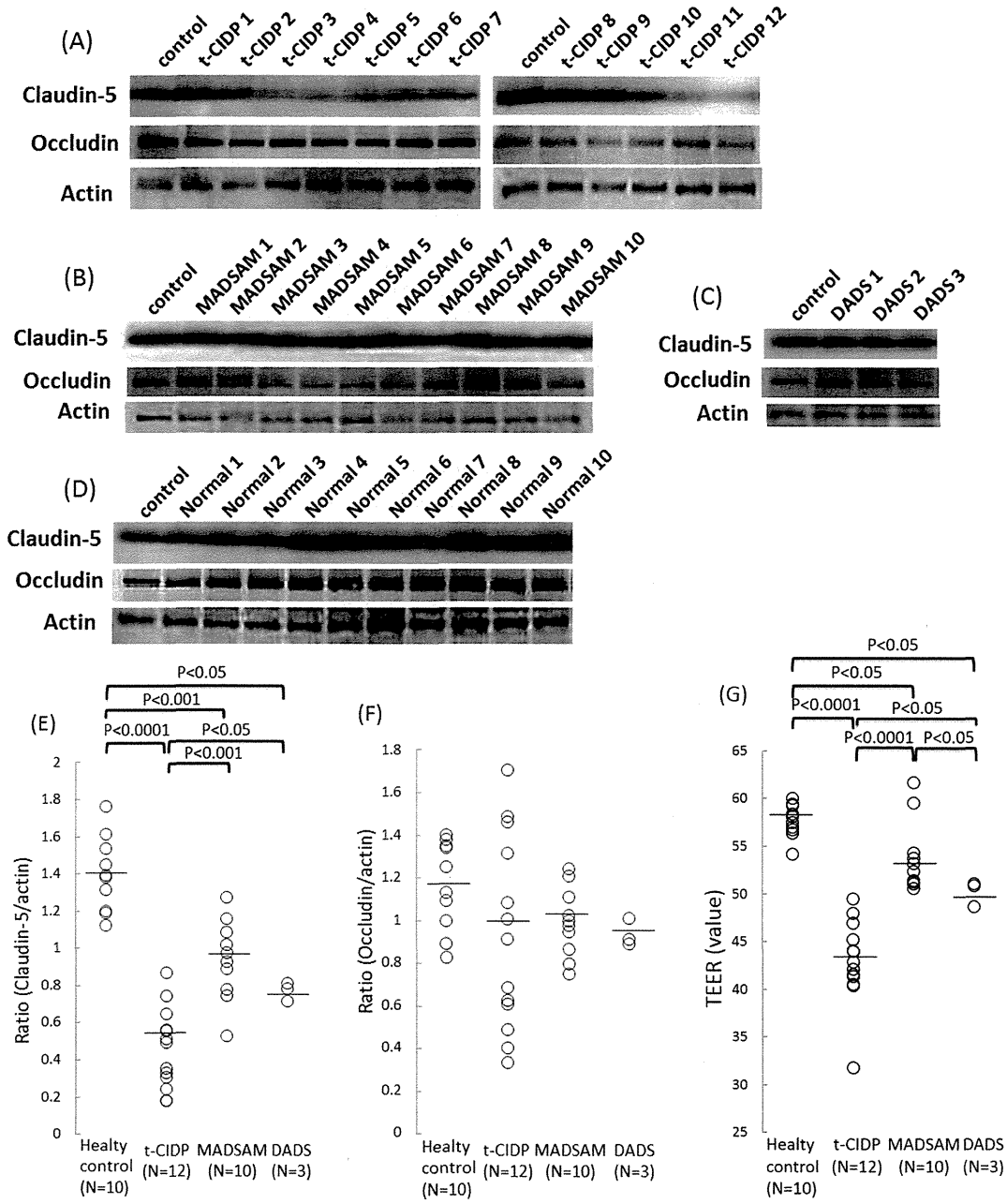

Figure 1. The sera obtained from the patients with t-CIDP, MADSAM and DADS disrupted the BNB. (A) – (D) Effects of the sera obtained from patients with three different phenotypes of chronic inflammatory demyelinating polyneuropathy (CIDP) on the protein levels of claudin-5 and occludin in the FH-BNBs, as determined using a Western blot analysis. The cells were exposed to sera from either patients with typical CIDP (t-CIDP) (A), multifocal acquired demyelinating sensory and motor neuropathy (MADSAM) (B) or distal acquired demyelinating symmetric neuropathy (DADS) (C) or healthy volunteers (D). (E) The sera obtained from the patients with t-CIDP, MADSAM neuropathy and DADS neuropathy decreased the protein ratio of claudin-5 to actin proteins in the FH-BNBs compared to that observed following exposure to the sera from the healthy volunteers. The decrease in the claudin-5 levels in the FH-BNBs was greater after incubation with the sera obtained from the t-CIDP patients than after that with the sera from the patients with MADSAM and DADS. (F) There were no significant differences between the patients with the three different phenotypes of CIDP and the healthy controls regarding the occludin protein levels in the FH-BNBs. (G) The effects of the sera on the transendothelial electrical resistance (TEER) values in the FH-BNBs were also evaluated. Adding sera obtained from the patients with t-CIDP, MADSAM neuropathy or DADS neuropathy resulted in decreased TEER values in the FH-BNBs in comparison with that observed in the cells treated with the sera obtained from the healthy volunteers. Markedly decreased TEER values in FH-BNBs were also observed in the FH-BNBs following incubation with the sera obtained from the t-CIDP patients compared to that noted in the cells incubated with sera from patients with MADSAM or DADS neuropathy. The TEER values were decreased following exposure to the sera obtained from the patients with DADS neuropathy compared to that observed after exposure to the sera obtained from the patients with MADSAM neuropathy. The bars indicate the mean level in each group. Control: non-conditioned DMEM containing 20% FBS. t-CIDP: conditioned medium with 10% sera obtained from patients with t-CIDP diluted with non-conditioned DMEM containing 10% FBS. MADSAM: conditioned medium with 10% sera obtained from patients with MADSAM diluted with non-conditioned DMEM containing 10% FBS. DADS: conditioned medium with 10% sera obtained from patients with DADS diluted with non-conditioned DMEM containing 10% FBS. Normal: conditioned medium with 10% sera obtained from a healthy volunteer diluted with non-conditioned medium of DMEM containing 10% FBS.
doi:10.1371/journal.pone.0104205.g001

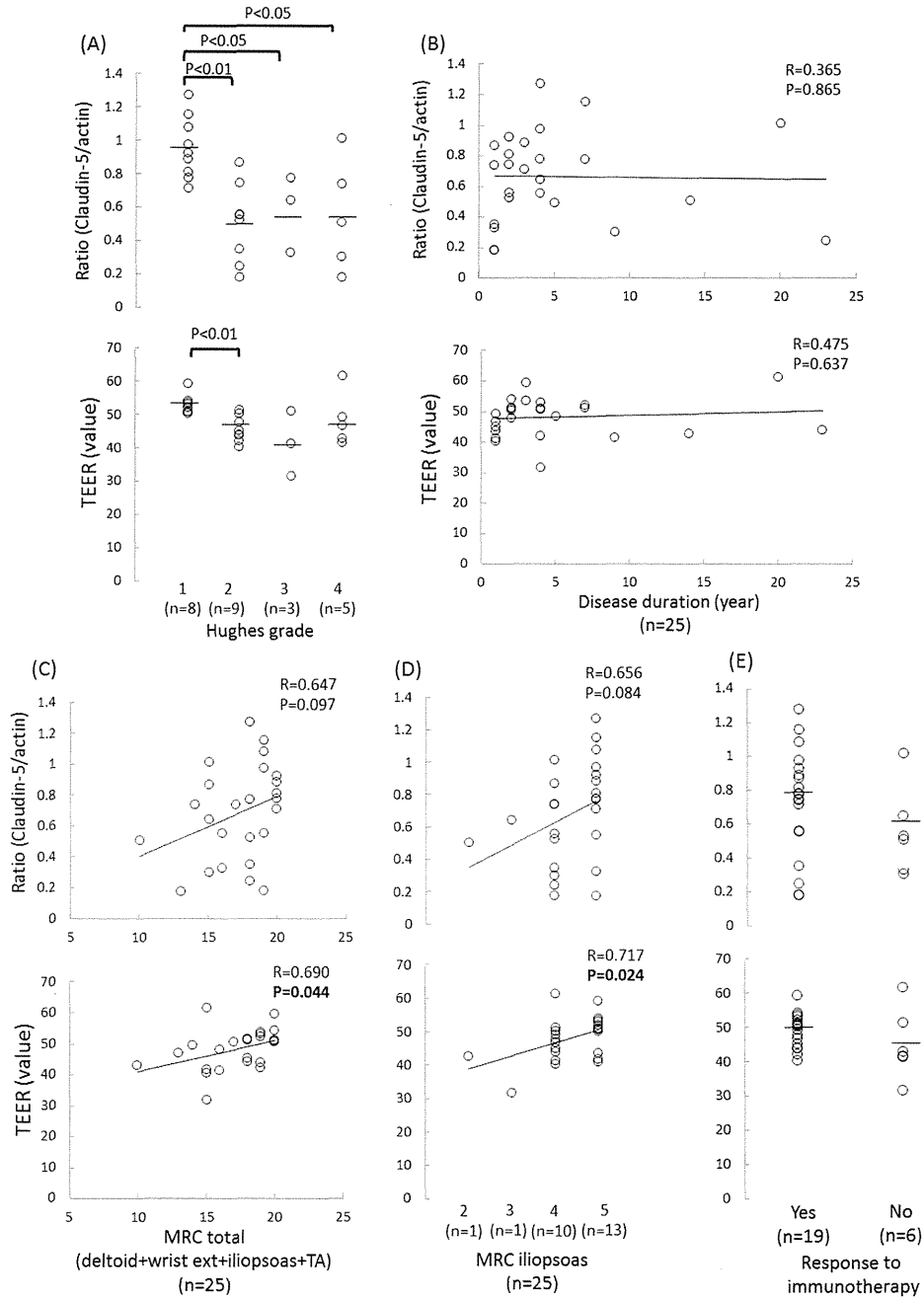

Figure 2. Associations between the clinical findings and BNB malfunction in the patients with CIDP. Correlations between the claudin-5 to actin protein ratios and the TEER values in the FH-BNBs following exposure to sera and the clinical parameters in the patients with CIDP. Associations between the claudin-5 to actin protein ratios and TEER values and the Hughes grade (A), duration of disease from onset (B), total Medical Research Council (MRC) scores for four muscle groups (deltoid, wrist extensor, iliopsoas, and tibialis anterior muscles) (C), MRC score for the iliopsoas muscle (D) and response to treatment, including intravenous immunoglobulin (IVIg) and corticosteroids (E). A lower ratio of claudin-5 to actin proteins was significantly associated with a higher Hughes grade, while a lower TEER value significantly correlated with a higher Hughes grade and lower MRC score.

doi:10.1371/journal.pone.0104205.g002

In addition, a lower ratio of claudin-5 to actin proteins significantly correlated with a higher Hughes grade (**Fig. 2A**) and higher Q Alb level (**Fig. 3C**), while a lower TEER value was significantly associated with a higher Hughes grade (**Fig. 2A**), lower MRC score (**Fig. 2C**), particularly in the iliopsoas muscle (**Fig. 2D**), more pronounced slowing of the motor nerve conduction in the median nerve (**Fig. 4B**) and higher frequency of abnormal temporal dispersion (**Fig. 4F**). In contrast, no significant differences were noted between the claudin-5 to actin protein ratio or TEER value and the duration of disease from onset (**Fig. 2B**), response to immunotherapy (**Fig. 2E**), concentration of CSF proteins (**Fig. 3A**), IgG index (**Fig. 3B**), distal latency (**Fig. 4A**),

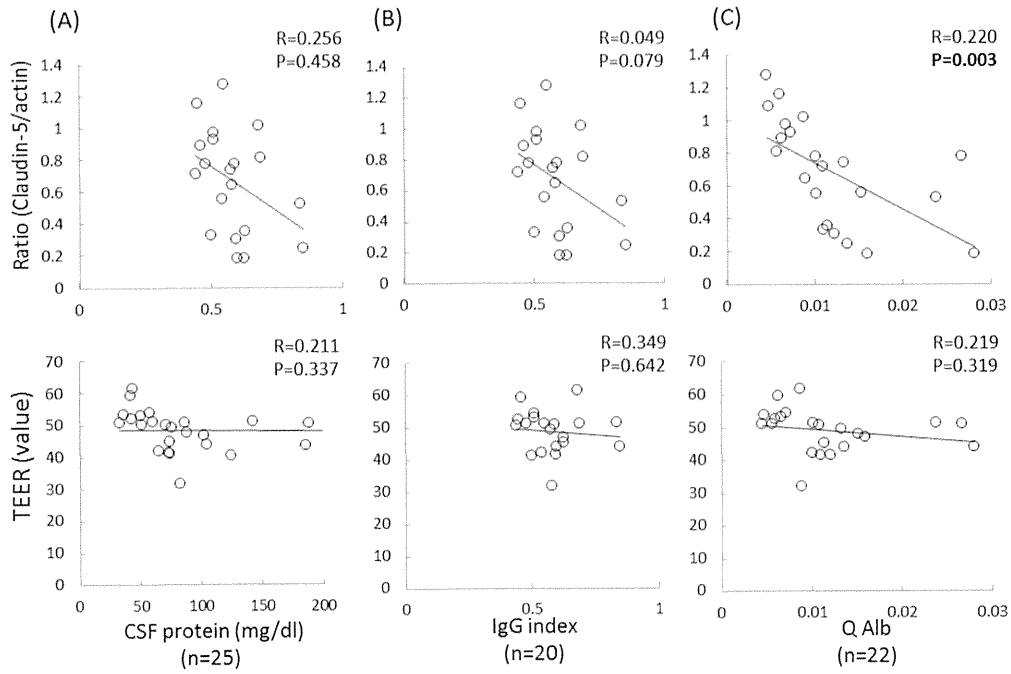

Figure 3. Associations between the CSF parameters and BNB disruption in the patients with CIDP. Correlations between the claudin-5 to actin protein ratios and the TEER values in the FH-BNBs following exposure to sera and the cerebrospinal fluid (CSF) parameters, including the CSF protein level (A), IgG index (B) and albumin ratio (Q Alb) (C) in the patients with CIDP. A lower ratio of claudin-5 to actin proteins was significantly associated with a higher Q Alb.
doi:10.1371/journal.pone.0104205.g003

conduction block (Fig. 4E) or CMAP amplitude (**Fig. 4C**) or TLI index (**Fig. 4D**) in the median nerve.

Discussion

According to the 2010 EFNS/PNS guidelines, CIDP comprises several clinical subtypes, including t-CIDP, MADSAM and DADS, based on the distribution of signs and symptoms [3]. Electrophysiological examinations provide important information regarding the pathogenesis of CIDP, as the distribution patterns of demyelinating lesions differ substantially between the different clinical phenotypes of CIDP [14]. These observations prompted us to hypothesize that differences in the patterns of BNB disruption at least partly determine the distribution of demyelinating lesions and clinical phenotypes of CIDP [10]. In cases of t-CIDP, motor nerve conduction studies frequently show a prolonged distal latency or duration of the distal CMAP, suggesting that demyelination predominantly may affect the distal nerve terminals, where the BNB is most vulnerable, during the initial phase of the disease [10,14]. However, demyelination also affects the intermediate nerve trunk after a long course of disease in individuals with t-CIDP, due to gradual disruption of the BNB in the nerve trunk. This phenomenon reflects profound slowing of nerve conduction, conduction block and/or abnormal temporal dispersion in the intermediate nerve segments, as identified on motor nerve conduction studies [10]. These disease processes suggest the importance of BNB breakdown in the development of t-CIDP. In contrast, electrophysiology studies of MADSAM have characterized the disease as involving multifocal nerve conduction block in the intermediate nerve trunks, with preservation of the nerve terminals and roots [10,19], suggesting the presence of multifocal demyelination in these regions. The pattern of BNB disruption appears to differ between MADSAM and t-CIDP, as the multifocal breakdown of the BNB at the site of conduction block may be required for the development of the former condition [10]. The hypothesis suggested by the findings of an electrophysiological studies is of great interest because it may explain the clinical variety of CIDP; however, it is not adequately supported by the results of pathological or cell biological examinations. Only one report regarding pathological changes in the endoneurial microvessels of patients with CIDP has been published to date [11]. This report described the characteristic of pathological changes in tight junction proteins, including a decrease in the level of claudin-5 and altered localization of ZO-1 on sural nerve biopsy samples obtained from t-CIDP patients. However, it remains unclear whether breakdown of the BNB is involved in the pathogenesis of atypical CIDP.

In the present study, we used our previous established human BNB-derived endothelial cells [16] and assessed the degree of BNB damage following exposure to sera by calculating the changes in the protein ratio of claudin-5 to actin proteins and measuring the TEER value [18]. Our results demonstrated that the sera obtained from the patients with three clinical phenotypes of CIDP all significantly decreased claudin-5 expression and the TEER value in the FH-BNBs, suggesting that humoral factors present in the sera of MADSAM and DADS patients, as well as t-CIDP patients, induce the BNB malfunction. The decrease in the claudin-5 protein level and TEER values observed following exposure to the sera obtained from the t-CIDP patients was more remarkable than that observed after incubation with the sera obtained from the patients with MADSAM or DADS. These findings indicate that the severity of BNB breakdown differs depending on the clinical phenotype of CIDP; humoral factors in the sera of t-CIDP patients may cause more severe BNB damage than those present in the

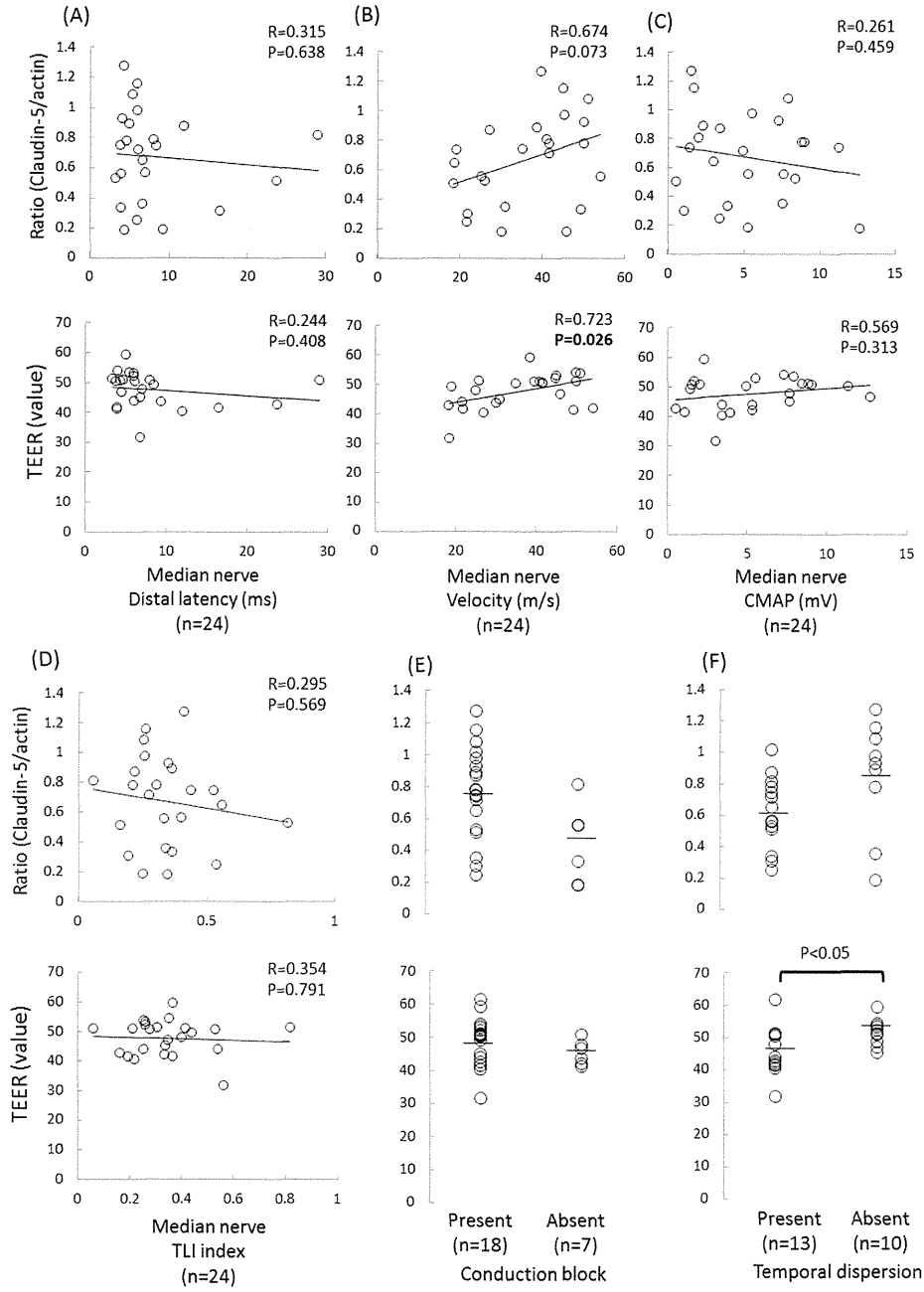

Figure 4. Correlation between the electrophysiological findings and BNB disruption in the patients with CIDP. Associations between the claudin-5 to actin protein ratios and the TEER values in the FH-BNBs following exposure to sera and the electrophysiological findings of the median nerve, including the distal nerve latency (A), conduction velocity (B), compound muscle action potential (CMAP) (C), terminal latency index (TLI index) (D) and presence of conduction block (E) or abnormal temporal dispersion (F) in the patients with CIDP. A lower TEER value was highly associated with slower motor nerve conduction and the presence of abnormal temporal dispersion.
doi:10.1371/journal.pone.0104205.g004

sera of patients with MADSAM or DADS. These results partly support the hypothesis suggested by the electrophysiological studies regarding the importance of BNB breakdown induced by humoral factors in t-CIDP sera.

We next examined the associations between the clinical, laboratory or electrophysiological findings and the degree of BNB damage following exposure to the sera obtained from the CIDP patients. Consequently, the severity of BNB damage after exposure to the sera significantly correlated with both a higher Hughes grade and lower MRC score, particularly in the iliopsoas muscle, which reflect the presence of clinical disability and proximal muscle weakness, respectively. Severe BNB breakdown was also found to be associated with a decrease in the speed of conduction in the median nerve in addition to abnormal temporal dispersion, thus indicating the presence of demyelination in the intermediate segments. Furthermore, this damage correlated with

an increased Q Alb value, which may reflect disruption of the BNB surrounding the nerve roots. Taken together, these findings suggest that the breakdown of the BNB induced by humoral factors in CIDP sera results in a wide range of symptoms of demyelination from the intermediate nerve trunk to the nerve root, and correlates with both clinical disability and proximal muscle weakness characteristics of t-CIDP. On the other hand, no associations were observed between impairment of the BNB and the duration of the disease or response to immunotherapy in the CIDP patients in our study. This finding suggests that BNB damage does not become more severe as the duration of disease increase, and that the extent of such damage cannot be used to predict the response to treatment.

Katz et al. reported that patients with demyelinating sensory polyneuropathy and distal weakness can be classified as having DADS, in order to distinguish the phenotype from t-CIDP [8]. In addition, two-thirds of patients with DADS have IgM monoclonal gammopathy, and the disease is usually associated with anti-MAG antibodies [20,21]. DADS associated with positivity for anti-MAG antibodies, termed anti-MAG neuropathy, is separated from CIDP according to the 2010 EFNS/PNS guidelines [3,22]. In contrast, DADS without anti-MAG antibodies is often considered to be a variant of CIDP, and some reports have described differences in the response to immune treatment between DADS patients with and without anti-MAG antibodies [23,24]. In the present study, we assessed the effects of sera obtained from three patients with DADS without anti-MAG antibodies, and found that the level of BNB damage after exposure to the sera from these patients was milder than that observed following exposure to the sera of the t-CIDP patients. In addition, we demonstrated a prolonged distal latency and smaller terminal latency index, both of which suggest preferential demyelination in the distal nerve terminals, to be more frequent in the patients with DADS, although these findings did not correlate with the severity of BNB damage. These results suggest that the phenotypic discrepancies observed between t-CIDP and DADS may be due to differences in the location of BNB breakdown; namely, the "DADS phenotype" may be associated with primary involvement at the distal nerve terminal with a vulnerable BNB, as the humoral factors in DADS sera do not induce substantial BNB malfunction at the nerve trunk, compared to that observed in the setting of t-CIDP.

Based on the hypothesis suggested by the finding of electrophysiological studies, the conduction block in the nerve trunk noted in patients with MADSAM is thought to always be accompanied by focal breakdown of the BNB [10]. However, our present results suggest that this conduction block may have little relationship with the involvement of the BNB induced by humoral immunity, as the BNB damage observed after exposure to the sera obtained from the MADSAM patients was milder than that detected after exposure to the sera obtained from the t-CIDP and DADS patients and the presence of conduction block did not correlate with the severity of BNB damage after exposure to sera from any of the patients. Nevertheless, due to the *in vitro* nature of our experiments, we were unable to fully estimate the importance of the BNB breakdown induced by cellular immunity in the MADSAM patients because our data could not be used to elucidate the contribution of the sera to the passage of inflammatory cells across the BNB. It is possible that focal BNB breakdown at site(s) of conduction block is involved in the pathophysiology of MADSAM via the up-regulation of inflammatory cytokines and adhesion molecules. Therefore, further studies to clarify the association between BNB damage and cellular immunity in the setting of MADSAM are required.

The clinical and electrophysiological features of MADSAM and multifocal motor neuropathy (MMN) are very similar, although MADSAM can be distinguished from MMN by the presence of overt sensory involvement, infrequency of anti-GM1 IgM autoantibodies and responsiveness to steroid treatment [6,25]. In addition, the severity of BNB breakdown appear to differ between the two diseases. We previously reported that the sera derived from MMN patients decrease the claudin-5 protein level and the TEER values in the BNB by approximately 50% compared to that observed in healthy controls based on the same *in vitro* BNB model [18]. Comparing the finding of our previous and present studies, BNB damage is more severe in patients with MMN than in those with MADSAM, suggesting that humoral factors play a greater role in the onset of MMN than in that of MADSAM. This hypothesis implies that the pathological mechanism underlying the development of MMN are significantly different from those of MADSAM, although the two diseases share similar clinical features.

In conclusion, the present findings suggest that the severity of BNB breakdown differs depending on the clinical phenotype of CIDP, and may be associated with both the clinical disability and demyelination in the nerve trunk. Our data imply that measurements of the degree of the BNB breakdown would be useful diagnostic biomarkers for predicting both the clinical phenotype and course of CIDP. However, because this was retrospective, further prospective, large-scale studies are required to validate our findings. The accumulation of further data regarding the molecular mechanism(s) responsible for the BNB impairment observed in patients with CIDP may also lead to the development of improved or novel treatments for CIDP.

Ethic approval

The study was approved by the ethics committee of Yamaguchi University.

Provenance and peer review

Not commissioned; externally peer reviewed.

Author Contributions

Conceived and designed the experiments: FS TK. Performed the experiments: FS YS HN. Analyzed the data: FS YS MK TK. Contributed reagents/materials/analysis tools: SS MB SM SK. Contributed to the writing of the manuscript: FS SK TK.

References

1. Vallat JM, Sommer C, Magy L (2010) Chronic inflammatory demyelinating polyradiculoneuropathy: diagnostic and therapeutic challenges for a treatable condition. Lancet Neurol 9: 402–412.
2. Hughes R (2010) Chronic Inflammatory Demyelinating Polyradiculoneuropathy. J Clin Immunol 30: S70–73.
3. Van den Bergh PY, Hadden RD, Bouche P, Cornblath DR, Hahn A, et al (2010) European Federation of Neurological Societies/Peripheral Nerve Society guideline on management of chronic inflammatory demyelinating polyradiculoneuropathy: report of a joint task force of the European Federation of Neurological Societies and the Peripheral Nerve Society - first revision. Eur J Neurol 17: 356–363.
4. (1991) Research criteria for diagnosis of chronic inflammatory demyelinating polyneuropathy (CIDP). Report from an Ad Hoc Subcommittee of the American Academy of Neurology AIDS Task Force. Neurology 41: 617–618.
5. Barohn RJ, Kissel JT, Warmolts JR, Mendell JR (1989) Chronic inflammatory demyelinating polyradiculoneuropathy. Clinical characteristics, course, and recommendations for diagnostic criteria. Arch Neurol 46: 878–884.

6. Saperstein DS, Amato AA, Wolfe GI, Katz JS, Nations SP, et al (1999) Multifocal acquired demyelinating sensory and motor neuropathy: the Lewis-Sumner syndrome. Muscle Nerve 22: 560–566.
7. Viala K, Renié L, Maisonobe T, Béhin A, Neil J, et al (2004) Follow-up study and response to treatment in 23 patients with Lewis-Sumner syndrome. Brain 127: 2010–2017.
8. Katz JS, Saperstein DS, Gronseth G, Amato AA, Barohn RJ (2000) Distal acquired demyelinating symmetric neuropathy. Neurology 54: 615–620.
9. Saperstein DS, Katz JS, Amato AA, Barohn RJ (2001) Clinical spectrum of chronic acquired demyelinating polyneuropathies. Muscle Nerve 24: 311–324.
10. Kuwabara S, Misawa S (2011) Chronic inflammatory demyelinating polyneuropathy: Clinical subtypes and their correlation with electrophysiology. Clin Exp Neuroimmunol 2: 41–48.
11. Kanda T, Numata Y, Mizusawa H (2004) Chronic inflammatory demyelinating polyneuropathy: decreased claudin-5 and relocated ZO-1. J Neurol Neurosurg Psychiatry 75: 765–769.
12. Kanda T (2013) Biology of the blood-nerve barrier and its alteration in immune mediated neuropathies. J Neurol Neurosurg Psychiatry 84: 208–212.
13. Ubogu EE (2013) The molecular and biophysical characterization of the human blood-nerve barrier: current concepts. J Vasc Res 50: 289–303.
14. Kuwabara S, Ogawara K, Misawa S, Mori M, Hattori T (2002) Distribution patterns of demyelination correlate with clinical profiles in chronic inflammatory demyelinating polyneuropathy. J Neurol Neurosurg Psychiatry 72: 37–42.
15. Kuwabara S, Misawa S, Mori M, Tamura N, Kubota M (2006) Long term prognosis of chronic inflammatory demyelinating polyneuropathy: a five year follow up of 38 cases. J Neurol Neurosurg Psychiatry 77: 66–70.
16. Abe M, Sano Y, Maeda T, Shimizu F, Kashiwamura Y, et al (2012) Establishment and characterization of human peripheral nerve microvascular endothelial cell lines: a new in vitro blood-nerve barrier (BNB) model. Cell Struct Funct 37: 89–100.
17. Hughes RA, Newsom-Davis JM, Perkin GD, Pierce JM (1978) Controlled trial prednisolone in acute polyneuropathy. Lancet 2: 750–753.
18. Shimizu F, Omoto M, Sano Y, Mastui N, Miyashiro A, et al (2014) Sera from patients with multifocal motor neuropathy disrupt the blood-nerve barrier. J Neurol Neurosurg Psychiatry 85: 526–537.
19. Magda P, Latov N, Brannagan TH 3rd, Goldfarb A, Chin RL, et al (2005) Multifocal acquired sensory and motor neuropathy: electrodiagnostic features. J Clin Neuromuscul Dis 7: 10–18.
20. Van den Berg L, Hays AP, Nobile-Orazio E, Kinsella LJ, Manfredini E, et al (1996) Anti-MAG and anti-SGPG antibodies in neuropathy. Muscle Nerve 19: 637–643.
21. Chassande B, Léger JM, Younes-Chennoufi AB, Bengoufa D, Maisonobe T, et al (1998) Peripheral neuropathy associated with IgM monoclonal gammopathy: correlations between M-protein antibody activity and clinical/electrophysiological features in 40 cases. Muscle Nerve 21: 55–62.
22. Hadden RD, Nobile-Orazio E, Sommer C, Hahn A, Illa I, et al (2006) European Federation of Neurological Societies/Peripheral Nerve Society guideline on management of paraproteinaemic demyelinating neuropathies: report of a joint task force of the European Federation of Neurological Societies and the Peripheral Nerve Society. Eur J Neurol 13: 809–818.
23. Larue S, Bombelli F, Viala K, Neil J, Maisonobe T, et al (2011) Non-anti-MAG DADS neuropathy as a variant of CIDP: clinical, electrophysiological, laboratory features and response to treatment in 10 cases. Eur J Neurol 18: 899–905.
24. Mygland A, Monstad P (2003) Chronic acquired demyelinating symmetric polyneuropathy classified by pattern of weakness. Arch Neurol 2003; 60: 260–264.
25. Katz JS, Saperstein DS (2001). Asymmetric Acquired Demyelinating Polyneuropathies: MMN and MADSAM. Curr Treat Options Neurol 3: 119–125.

ARTHRITIS & RHEUMATOLOGY
Vol. 66, No. 7, July 2014, pp 1864–1871
DOI 10.1002/art.38630

A Crucial Role of L-Selectin in C Protein–Induced Experimental Polymyositis in Mice

Kyosuke Oishi,[1] Yasuhito Hamaguchi,[1] Takashi Matsushita,[1] Minoru Hasegawa,[1] Naoko Okiyama,[2] Jens Dernedde,[3] Marie Weinhart,[4] Rainer Haag,[4] Thomas F. Tedder,[5] Kazuhiko Takehara,[1] Hitoshi Kohsaka,[2] and Manabu Fujimoto[1]

Objective. **To investigate the role of adhesion molecules in C protein–induced myositis (CIM), a murine model of polymyositis (PM).**

Methods. **CIM was induced in wild-type mice, L-selectin–deficient (L-selectin$^{-/-}$) mice, intercellular adhesion molecule 1 (ICAM-1)–deficient (ICAM-1$^{-/-}$) mice, and mice deficient in both L-selectin and ICAM-1 (L-selectin$^{-/-}$ICAM-1$^{-/-}$ mice). Myositis severity, inflammatory cell infiltration, and messenger RNA expression in the inflamed muscles were analyzed. The effect of dendritic polyglycerol sulfate, a synthetic inhibitor that suppresses the function of L-selectin and endothelial P-selectin, was also examined.**

Results. **L-selectin$^{-/-}$ mice and L-selectin$^{-/-}$ ICAM-1$^{-/-}$ mice developed significantly less severe myositis compared to wild-type mice, while ICAM-1 deficiency did not inhibit the development of myositis. L-selectin$^{-/-}$ mice that received wild-type T cells developed myositis. Treatment with dendritic polyglycerol sulfate significantly diminished the severity of myositis in wild-type mice compared to treatment with control.**

Conclusion. **These data indicate that L-selectin plays a major role in the development of CIM, whereas ICAM-1 plays a lesser role, if any, in the development of CIM. L-selectin–targeted therapy may be a candidate for the treatment of PM.**

Polymyositis (PM) is a chronic autoimmune inflammatory myopathy. It affects striated muscles and induces varying degrees of weakness, especially in the proximal muscles (1). Although the pathogenesis of PM has not been elucidated, cytotoxic CD8+ T cells are thought to play a prominent role in the development of myositis (2). Recently, the C protein–induced myositis (CIM) model was established as an animal model of PM (3). The skeletal muscle C protein is a myosin-binding protein that regulates muscle filament components (4). This murine myositis is readily induced by a single immunization with recombinant skeletal muscle C protein fragments in C57BL/6 mice. CIM elicits abundant perforin-positive CD8+ T cells that infiltrate endomysial sites. In addition, CD8+ T cell depletion inhibits the progression of myositis. In the CIM model, inflammatory cytokines, including interleukin-1 (IL-1), IL-6, and tumor necrosis factor α (TNFα), mediate the induction and development of myositis (3,5,6). The CIM model is primarily used to examine the inflammatory phase of PM.

Leukocyte recruitment into sites of inflammation is accomplished by constitutive or inducible expression of multiple adhesion molecules (7–9). L-selectin (CD62L), which primarily mediates leukocyte capture and rolling on the endothelium, is constitutively expressed by most leukocytes (10). In addition, L-selectin plays significant roles in the activation of multiple intracellular signaling pathways (11). Intercellular adhesion

Supported by the Ministry of Health, Labor, and Welfare of Japan and the Ministry of Education, Culture, Sports, Science, and Technology of Japan (intractable diseases research grant), the DFG (grant to the Collaborative Research Center SFB 765), and the NIH (grant AI-056363 to Dr. Tedder).

[1]Kyosuke Oishi, MD, Yasuhito Hamaguchi, MD, PhD, Takashi Matsushita, MD, PhD, Minoru Hasegawa, MD, PhD, Kazuhiko Takehara, MD, PhD, Manabu Fujimoto, MD: Kanazawa University, Kanazawa, Japan; [2]Naoko Okiyama, MD, PhD, Hitoshi Kohsaka, MD, PhD: Tokyo Medical and Dental University, Tokyo, Japan; [3]Jens Dernedde, PhD: Charité–Universitätsmedizin Berlin, Berlin, Germany; [4]Marie Weinhart, PhD, Rainer Haag, PhD: Freie Universität, Berlin, Germany; [5]Thomas F. Tedder, PhD: Duke University Medical Center, Durham, North Carolina.

Address correspondence to Yasuhito Hamaguchi, MD, PhD, Department of Dermatology, Faculty of Medicine, Institute of Medical, Pharmaceutical, and Health Sciences, Kanazawa University, 13-1 Takaramachi, Kanazawa, Ishikawa 920-8641, Japan. E-mail: yasuhito@med.kanazawa-u.ac.jp.

Submitted for publication July 16, 2013; accepted in revised form March 11, 2014.

molecule 1 (ICAM-1; CD54) is a member of the Ig superfamily that is constitutively expressed on endothelial cells, subsets of leukocytes, fibroblasts, and epithelial cells (12). It can be transcriptionally up-regulated by several proinflammatory cytokines, such as TNFα, interferon-γ (IFNγ), and IL-1 (12). L-selectin and ICAM-1 act in concert with each other during leukocyte migration from blood to extravascular tissues where inflammatory responses occur in vivo (13,14).

The relative contributions of L-selectin and ICAM-1 are largely dependent on the type of model of inflammation being used. For instance, in the immediate-type hypersensitivity model, deficiency of either L-selectin or ICAM-1 resulted in the immune response being reduced to similar degrees. Deficiency of both L-selectin and ICAM-1 did not exhibit a synergistic effect (15). Introducing defective ICAM-1 into L-selectin–deficient (L-selectin$^{-/-}$) mice resulted in a profoundly decreased pulmonary fibrosis compared to that observed in mice with a deficiency of a single adhesion molecule in a bleomycin-induced pulmonary fibrosis model (16). However, wound healing was not inhibited by L-selectin deficiency, while delayed wound healing was observed in ICAM-1-deficient (ICAM-1$^{-/-}$) mice (17). Nevertheless, the relative contributions and interaction of L-selectin and ICAM-1 in the CIM model remain unknown.

In this study, we investigated the role of adhesion molecules in CIM by using L-selectin$^{-/-}$ mice, ICAM-1$^{-/-}$ mice, and L-selectin and ICAM-1 double-deficient (L-selectin$^{-/-}$ICAM-1$^{-/-}$) mice. Inhibition of L-selectin ameliorated the severity of myositis. The results of this study indicate that L-selectin contributes to the development of CIM more than ICAM-1 does, and that L-selectin might serve as a therapeutic target for the treatment of PM.

MATERIALS AND METHODS

Mice. L-selectin$^{-/-}$ mice were produced as previously described (18). ICAM-1$^{-/-}$ mice (19) were from The Jackson Laboratory, and L-selectin$^{-/-}$ICAM-1$^{-/-}$ mice were generated as previously described (14). All mice were backcrossed more than 8 generations onto the C57BL/6 genetic background. Female mice ages 8–10 weeks were used in the experiments. Age-matched C57BL/6 mice (The Jackson Laboratory) were used as controls. All mice were housed in a specific pathogen–free barrier facility and screened regularly for pathogens. The Committee on Animal Experimentation of Kanazawa University Graduate School of Medical Science approved all studies and procedures.

CIM induction. To induce CIM, 8–10-week-old female mice were immunized intradermally with 200 μg of murine C protein fragments (3) emulsified in 200 μl of Freund's complete adjuvant (CFA) containing 100 μg of heat-killed *Mycobacterium butyricum* (Difco) (5). The immunogens were injected at multiple sites in the back and footpads. Pertussis toxin (0.2–2 μg; Seikagaku) in phosphate buffered saline (PBS) was injected intraperitoneally at the same time.

Mice were killed on day 14 after immunization with C protein, and muscle tissue specimens were harvested. Hematoxylin and eosin (H&E)–stained 10-μm sections of the hamstrings and quadriceps were examined histologically. The histologic severity of myositis in each muscle block was graded (3) on a scale of 1–4, where 1 = involvement of $\geq$1 muscle fiber but <5 muscle fibers, 2 = a lesion involving 5–30 muscle fibers, 3 = a lesion involving a muscle fasciculus, and 4 = diffuse, extensive lesions. When multiple lesions with the same grade were found in a single muscle block, 0.5 was added to the grade. We also assessed necrotic muscle areas. Necrotic muscle areas were quantified by measuring necrotic muscle fibers showing decreased H&E staining and the replacement of muscle fibers by mononuclear cell infiltrates (6).

Immunohistochemical staining. Muscle sections (4 μm thick) obtained from the left thighs of the mice were frozen in cold 2-methylbutane and were stained with anti-CD8a (53-6.7) and anti-CD4 (RM4-5) (BD Biosciences). Muscle sections (4 μm thick) obtained from the right thighs of the mice were fixed in formalin, dehydrated, embedded in paraffin, and then incubated with rat monoclonal antibodies specific for CD3 (CD3-12; Serotec), F4/80 (A3-1; Abcam), and myeloperoxidase (MPO; NeoMarkers). Six inflammatory mononuclear cell foci in the serial sections were studied. Stained cells were counted in every focus under high magnification (400×) using a light microscope. The mean score was used for analysis. The stained sections were evaluated by 2 independent observers who reported comparable results.

Adoptive transfer of mouse spleen T cells. Single-cell suspensions of splenic leukocytes from naive, nonimmunized wild-type mice were generated by gentle homogenization. CD90.2 monoclonal antibody–coupled microbeads were used to purify T cell populations according to the recommendations of the manufacturer (Miltenyi Biotech). The purity of extracted T cells from donor mice was measured using a FACSCanto II flow cytometer (BD Biosciences), and purities were >90%. Viable spleen T cells (8×10^6) were transferred intravenously into recipient L-selectin$^{-/-}$ mice. Twenty-four hours after adoptive transfer of T cells, recipient L-selectin$^{-/-}$ mice were immunized with C protein fragments, and 14 days after immunization their muscles were harvested as described above. PBS-injected mice were used as controls.

Real-time reverse transcription–polymerase chain reaction (RT-PCR). Total RNAs were extracted from muscle samples using Qiagen RNeasy spin columns, and real-time RT-PCR was performed using a TaqMan system (Applied Biosystems) on an ABI Prism 7000 Sequence Detector (Applied Biosystems) (20). TaqMan probes and primers for IL-1β, IL-6, IL-10, IL-12α, IFNγ, TNFα, monocyte chemoattractant protein 1 (MCP-1), and GAPDH were purchased from Applied Biosystems. Relative expression of RT-PCR products was determined using the $\Delta\Delta C_t$ technique. Each reaction was performed at least in triplicate.

Treatment of mice with dendritic polyglycerol sulfate. Dendritic polyglycerol sulfates are multivalent inhibitors of

inflammation that inhibit both L-selectin and endothelial P-selectin with high efficacy (21). Wild-type mice were injected subcutaneously with dendritic polyglycerol sulfate (0.3 mg/mouse) into the shaved neck for 11 consecutive days, beginning 3 days after immunization with C protein. Mice injected subcutaneously with PBS were used as controls.

Statistical analysis. The Mann-Whitney U test was used to determine the level of significance of differences in the sample means. The Bonferroni test was used for multiple comparisons. All statistical analysis was performed using Prism software.

RESULTS

Amelioration of myositis severity in L-selectin–deficient mice. To determine if adhesion molecules play a role in myositis, we assessed the severity of myositis in wild-type, L-selectin$^{-/-}$, ICAM-1$^{-/-}$, and L-selectin$^{-/-}$ ICAM-1$^{-/-}$ mice (Figure 1A). Histologic scores were significantly lower in L-selectin$^{-/-}$ mice than in wild-type mice ($P < 0.01$) (Figure 1B). Similarly, ICAM-1$^{-/-}$ mice demonstrated a 50% decrease in myositis severity score compared to wild-type mice, although the differences did not reach significance. L-selectin$^{-/-}$ ICAM-1$^{-/-}$ mice displayed significantly lower histologic scores compared to wild-type mice ($P < 0.01$). Histologic scores in L-selectin$^{-/-}$ and L-selectin$^{-/-}$ ICAM-1$^{-/-}$ mice were also significantly lower than those in ICAM-1$^{-/-}$ mice ($P < 0.01$ for both).

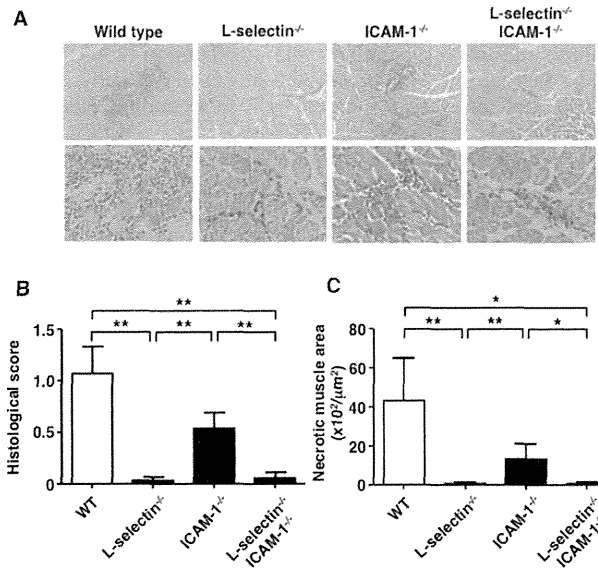

Figure 1. C protein–induced myositis in wild-type (WT) mice, L-selectin–deficient mice, ICAM-1–deficient mice, and mice deficient in both L-selectin and ICAM-1. Mice were killed on day 14 after immunization with C protein, and muscle tissue specimens were harvested. **A,** Representative images of muscle inflammation in the indicated mouse genotypes. Hematoxylin and eosin stained. Original magnification × 100 in top panels; × 400 in bottom panels. **B** and **C,** Histologic score (**B**) and area of muscle fiber necrosis (**C**) in each mouse group. Bars show the mean ± SEM (n = 8–10 mice per genotype). * = $P < 0.05$; ** = $P < 0.01$.

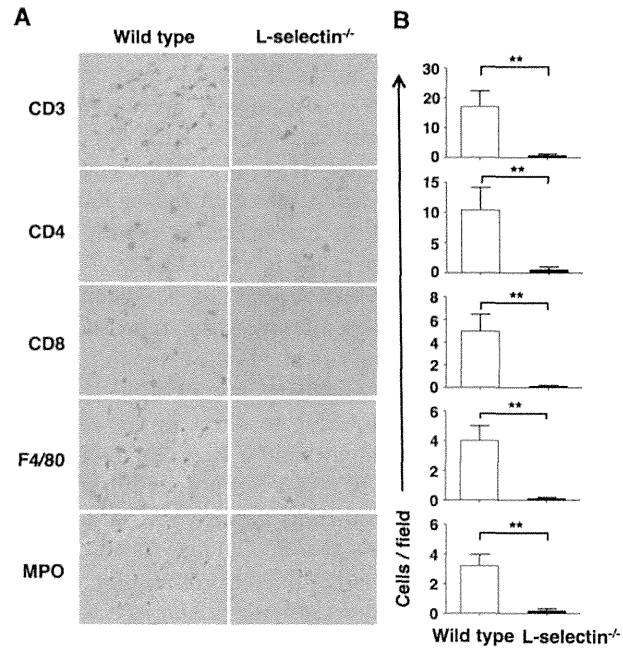

Figure 2. Inflammatory cell infiltration into the inflamed muscles of wild-type and L-selectin$^{-/-}$ mice with C protein–induced myositis. Mice were killed on day 14 after immunization with C protein, and muscle tissue specimens were harvested. **A,** Representative immunohistochemical images showing CD3, CD4, CD8, F4/80, and myeloperoxidase (MPO) staining in tissue sections from wild-type and L-selectin$^{-/-}$ mice. *Original magnification* × 400. **B,** Numbers of CD3+, CD4+, and CD8+ T cells, F4/80-positive macrophages, and MPO-positive neutrophils in wild-type and L-selectin$^{-/-}$ mice on day 14. Bars show the mean ± SEM (n = 8–10 mice per genotype). ** = $P < 0.01$.

We also assessed necrotic muscle areas to evaluate muscle damage in the mice (Figure 1C). Necrotic muscle areas were significantly smaller in L-selectin$^{-/-}$ mice than in wild-type mice ($P < 0.01$). ICAM-1$^{-/-}$ mice showed a 69% decrease in necrotic muscle areas compared to wild-type mice. L-selectin$^{-/-}$ICAM-1$^{-/-}$ mice displayed significantly decreased necrotic muscle areas comparable to those of L-selectin$^{-/-}$ mice. Necrotic muscle areas in L-selectin$^{-/-}$ and L-selectin$^{-/-}$ ICAM-1$^{-/-}$ mice were also significantly smaller than those in ICAM-1$^{-/-}$ mice ($P < 0.01$ and $P < 0.05$, respectively). Histologic scores paralleled the increases in necrotic muscle areas. L-selectin$^{-/-}$ and L-selectin$^{-/-}$

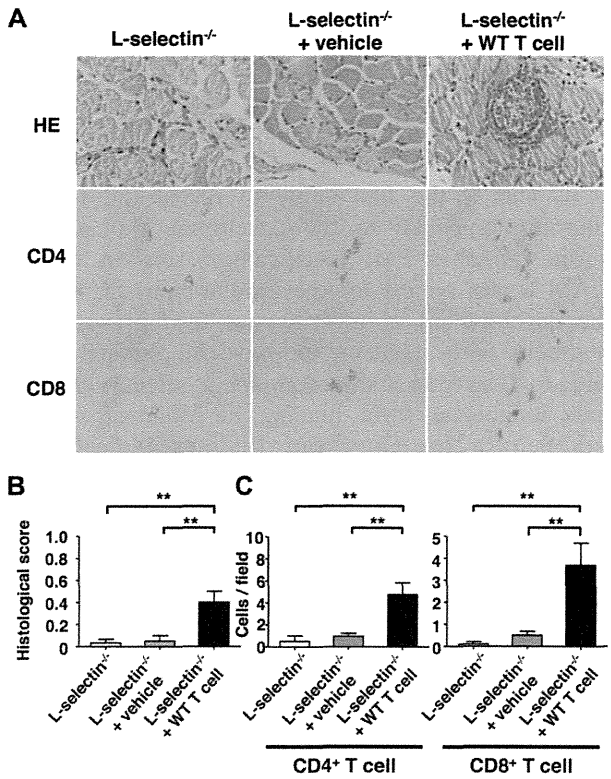

Figure 3. Adoptive transfer of T cells from wild-type (WT) mice into L-selectin$^{-/-}$ mice. Mice were killed on day 14 after immunization with C protein, and muscle tissue specimens were harvested. **A,** Representative muscle sections stained with hematoxylin and eosin (H&E) and immunohistochemical images showing CD4 and CD8 staining in sections from L-selectin$^{-/-}$ mice, L-selectin$^{-/-}$ mice treated with vehicle, and L-selectin$^{-/-}$ mice that received wild-type T cells. Original magnification × 400. **B,** Histologic score in each mouse group. **C,** Numbers of CD4+ and CD8+ T cells. Bars in **B** and **C** show the mean ± SEM (n = 5 mice per group). ** = $P < 0.01$.

ICAM-1$^{-/-}$ mice developed a minimal degree of myositis. These results suggest that L-selectin contributes profoundly to the development of CIM, whereas the contribution of ICAM-1 is less relevant.

Reduced leukocyte recruitment in L-selectin–deficient mice. Since L-selectin$^{-/-}$ mice, but not ICAM-1$^{-/-}$ mice, showed significantly less severe myositis compared to wild-type mice, we assessed inflammatory cell infiltration in the inflamed muscles of wild-type mice and L-selectin$^{-/-}$ mice (Figures 2A and B). Immunohistologic staining revealed that CD3+, CD4+, and CD8+ T cells, F4/80-positive macrophages, and MPO-positive neutrophils were all significantly reduced in L-selectin$^{-/-}$ mice compared to wild-type mice ($P < 0.01$ for all comparisons). We detected very few B220+ B cells in the inflamed muscles of either wild-type mice or L-selectin$^{-/-}$ mice (data not shown). These results suggest that L-selectin plays an important role in the migration of leukocytes into inflamed muscles in the CIM model.

Development of myositis in L-selectin$^{-/-}$ mice that received wild-type T cells. Although L-selectin is expressed on various leukocyte subsets, CD8+ T cells are considered to be crucial for the induction of CIM. Therefore, we performed adoptive transfer experiments to confirm the importance of L-selectin expression on T cells. As described above, L-selectin$^{-/-}$ mice exhibited minimal development of myositis. In contrast, L-selectin$^{-/-}$ mice that received T cells from naive, nonimmunized wild-type mice developed readily apparent myositis. Histologic scores in L-selectin$^{-/-}$ mice that received wild-type T cells were ~10-fold higher than those of L-selectin$^{-/-}$ mice and L-selectin$^{-/-}$ mice treated with vehicle ($P < 0.01$ for both) (Figures 3A and B). Although the histologic scores in L-selectin$^{-/-}$ mice that received wild-type T cells were 52% lower than those in wild-type mice, the difference did not reach significance. Our analysis of cell infiltration showed that both CD4+ and CD8+ T cells were more abundant in L-selectin$^{-/-}$ mice that received wild-type T cells (Figure 3C). These results indicate that L-selectin expression on T cells is important for leukocyte migration into inflamed muscles and the development of myositis in mice.

Cytokine expression in CIM. We next compared messenger RNA (mRNA) expression in inflamed muscles from wild-type and L-selectin$^{-/-}$ mice by RT-PCR (Figure 4). The levels of mRNA for IL-6, IL-10, IL-12,

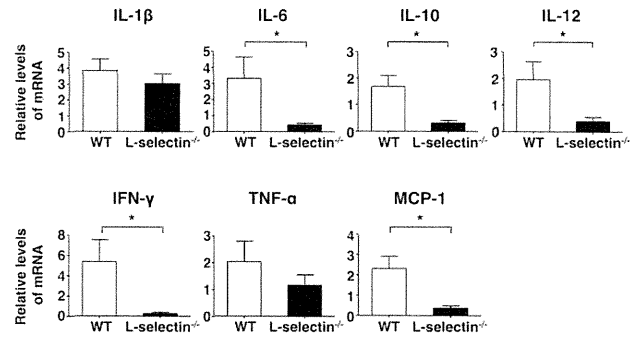

Figure 4. Levels of mRNA in the inflamed muscles from wild-type (WT) and L-selectin$^{-/-}$ mice on day 14 after immunization with C protein. Bars show the mean ± SEM (n = 5 or more mice per genotype). * = $P < 0.05$. IL-1β = interleukin-1β; IFNγ = interferon-γ; TNFα = tumor necrosis factor α; MCP-1 = monocyte chemoattractant protein 1.

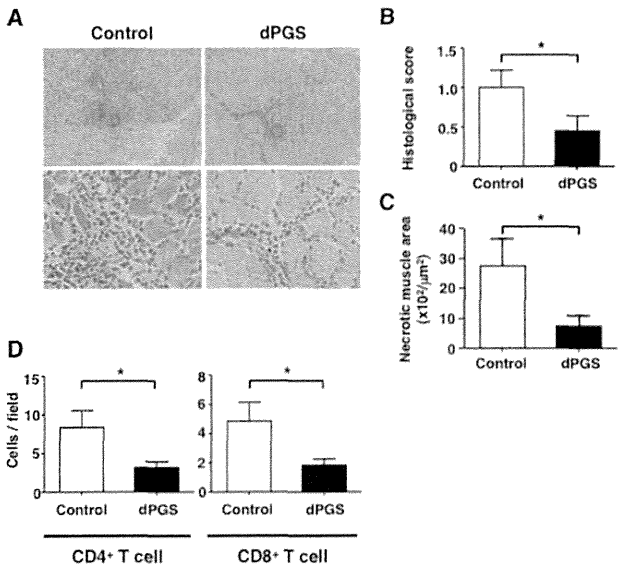

Figure 5. Decreased severity of myositis in wild-type mice treated with dendritic polyglycerol sulfate (dPGS). Dendritic polyglycerol sulfate was injected into mice intradermally for 11 consecutive days, beginning 3 days after immunization with C protein. Mice were killed on day 14 after immunization, and muscle tissue specimens were harvested. **A,** Representative images of muscle inflammation in wild-type mice treated with dendritic polyglycerol sulfate or phosphate buffered saline (control). Hematoxylin and eosin stained. Original magnification × 100 in top panels; × 400 in bottom panels. **B** and **C,** Histologic scores (**B**) and area of muscle fiber necrosis (**C**) in each mouse group. **D,** Numbers of CD4+ and CD8+ T cells on day 14. Bars in **B–D** show the mean ± SEM (n = 8–10 mice per group). * = $P < 0.05$.

IFNγ, and MCP-1 were significantly reduced in L-selectin$^{-/-}$ mice compared to wild-type mice ($P < 0.05$ for all comparisons). IL-1β and TNFα mRNA expression levels in L-selectin$^{-/-}$ mice were decreased 21% and 43%, respectively, compared to wild-type mice, but the differences did not reach significance for either cytokine.

Diminished severity of myositis in mice treated with dendritic polyglycerol sulfate. Since dendritic polyglycerol sulfate is an inhibitor that suppresses the function of adhesion molecules, including L-selectin, wild-type mice were treated with dendritic polyglycerol sulfate. Wild-type mice treated with dendritic polyglycerol sulfate showed 52% lower histologic scores than PBS-treated control wild-type mice ($P < 0.05$) (Figures 5A and B). Necrotic tissue areas from wild-type mice treated with dendritic polyglycerol sulfate were significantly smaller than those from PBS-treated control wild-type mice ($P < 0.05$) (Figure 5C). Infiltration of both CD4+ and CD8+ T cells was also significantly decreased by dendritic polyglycerol sulfate treatment (Figure 5D).

DISCUSSION

This is the first study to reveal the roles of adhesion molecules in the development of CIM, a murine model of PM. Specifically, L-selectin, but not ICAM-1, was critical for the development of myositis. The development of myositis was also prevented by treatment with dendritic polyglycerol sulfate, which binds to L-selectin and endothelial P-selectin and prevents leukocytes from binding to inflamed vascular endothelia (21). Thus, our findings indicate that L-selectin plays a critical role in the development of CIM, and that L-selectin could be a target for the treatment of PM.

The cell adhesion molecules L-selectin and ICAM-1 act cooperatively to mediate optimal leukocyte rolling and the recruitment of leukocytes to sites of inflammation (13,14,22–24). Although the relative contributions of L-selectin and ICAM-1 vary among different models of inflammation, ICAM-1 appears to play a more predominant role than L-selectin in general. However, this study indicates that L-selectin is more important than ICAM-1 in the development of CIM (Figures 1A and B).

Previous studies clearly indicate that CD8+ T cells play a more significant role than CD4+ T cells in the development of CIM. Tang et al (25) reported that the percentage of L-selectin–positive cells in CD8+ T cells was greater than that in CD4+ T cells, especially in lymphoid tissues, and that L-selectin expression levels were higher on CD8+ T cells than on CD4+ T cells in wild-type mice. In contrast, L-selectin deficiency did not affect ICAM-1 expression (16). Thus, the different expression levels of L-selectin between CD4+ and CD8+ T cells may partly explain the finding that L-selectin deficiency had a greater effect on the degree of myositis than ICAM-1 did in the present study. Alternatively, the greater role of L-selectin may be explained by the fact that L-selectin is important for antiviral immunity (26) and antitumor activity (27), in which CD8+ cytotoxic T cells play a substantial role. The etiologic role of CD8+ cytotoxic T cells may be another reason why L-selectin is more important than ICAM-1 in the CIM model.

It is assumed that leukocyte infiltration and cytokines participate in the development of CIM. Consistent with this, L-selectin$^{-/-}$ mice exhibited significantly decreased numbers of leukocytes, including CD4+ and

CD8+ T cells, F4/80-positive macrophages, and MPO-positive neutrophils, in the inflamed muscles on day 14 following CIM induction (Figures 2A and B). In addition, adoptive transfer of wild-type T cells induced myositis in L-selectin$^{-/-}$ mice (Figures 3A–C). These data suggest that L-selectin expression on T cells is required for the induction of myositis via the recruitment of leukocytes into the muscles. However, alternatives should be considered to explain the reduction in myositis severity seen in L-selectin$^{-/-}$ mice. It has been reported that myositis development required both the activation of T cells and the conditioning of local muscle tissue as a "seed and soil" model, and CIM regression was due to attenuation of local CFA-induced immune activation (28). Thus, local immune activation in L-selectin$^{-/-}$ mice might be impaired, leading to reduced myositis severity.

L-selectin expression on leukocytes may be important not only for leukocyte infiltration, but also for subsequent cytokine production. In the CIM model, IL-6 deficiency inhibited the progression of myositis, and IL-6 blockade reduced the severity of myositis (5). Consistent with this previous report, our study showed that IL-6 mRNA expression in the inflamed muscles of L-selectin$^{-/-}$ mice was significantly decreased compared to that in wild-type mice (Figure 4). Moreover, other inflammatory cytokines, including IL-12 and IFNγ, were decreased in L-selectin$^{-/-}$ mice as well. The incidence of myositis in IL-1–deficient and TNFα-deficient mice was significantly lower than that in wild-type mice (3). Although the differences did not reach significance, IL-1β and TNFα tended to decrease in L-selectin$^{-/-}$ mice compared to wild-type mice in this study (Figure 4). Taken together, these findings indicate that L-selectin expression influences cytokine production in inflamed mouse muscles. However, the mechanism by which L-selectin is involved in cytokine regulation needs to be evaluated.

The establishment of effective PM therapies has long been awaited. Corticosteroids have been proven to be beneficial, but serious adverse effects can frequently occur. To date, several studies targeting adhesion molecules have been performed. Bimosiamose is a small-molecule and pan-selectin antagonist that targets E-selectin, P-selectin, and L-selectin (29). Inhaled administration of bimosiamose in asthmatic patients was shown to attenuate late asthmatic reactions (30). Subcutaneous administration of bimosiamose improved the clinical scores in patients with psoriasis (31). A humanized anti–L-selectin monoclonal antibody (aselizumab) significantly increased survival time and decreased mortality in a baboon model of hemorrhagic-traumatic shock (32). However, intravenous administration of aselizumab to multiple traumatized patients resulted in no significant improvement of efficacy in a phase II clinical trial (33). Also, caution should be paid in developing biologic therapies targeting adhesion molecules. A humanized anti-CD11a monoclonal antibody, efalizumab, was effective for the treatment of psoriasis, but a long-term followup study revealed several fatal cases of progressive multifocal leukoencephalopathy by JC virus (34), leading to voluntary withdrawal of the drug from the market. In this study, the synthetic compound dendritic polyglycerol sulfate, which is an inhibitor that suppresses the function of leukocytic L-selectin and endothelial P-selectin, improved myositis severity (Figures 5A–C). Therefore, we assume that a selectin-targeted therapy could still be an option for the treatment of PM.

We are well aware that our study is impacted by a number of limitations. First, the murine CIM model of PM that was used only mimics the inflammatory aspect of the human disease. Second, immune responses against C protein have not been reported in human PM patients. Third, we did not conduct functional assays to directly assess muscle weakness in this study. In previous experiments, we attempted several assays, including a rotarod performance test and the measurement of serum creatinine kinase. We used rotarod tests in a previous study (3). However, according to our experience, the rotarod test turned out to be less reliable than histologic analyses, because mice learn how to avoid falling off and do not necessarily run consistently. In addition, serum levels of creatinine kinase or other muscle-derived proteins are unreliable parameters. They are often high in normal mice, presumably because of their physical activity (28). Devices are needed to directly quantify rodent muscle strength to best observe the clinical course of the disease.

In conclusion, immune cell infiltration initiated via selectin–ligand interactions and the production of proinflammatory cytokines, such as IL-6, and chemoattractants for inflammatory cells, such as MCP-1, may be a trigger of myositis in CIM. Our findings also indicate that the cell adhesion molecule L-selectin may be a candidate for treating PM, an intractable autoimmune disease.

ACKNOWLEDGMENTS

We thank Ms E. Yoshimoto, Ms M. Matsubara, and Ms Y. Yamada for technical assistance.

AUTHOR CONTRIBUTIONS

All authors were involved in drafting the article or revising it critically for important intellectual content, and all authors approved the final version to be published. Dr. Hamaguchi had full access to all of the data in the study and takes responsibility for the integrity of the data and the accuracy of the data analysis.

Study conception and design. Oishi, Hamaguchi, Kohsaka, Fujimoto.
Acquisition of data. Oishi, Hamaguchi, Dernedde, Weinhart, Haag, Tedder, Kohsaka.
Analysis and interpretation of data. Oishi, Hamaguchi, Matsushita, Hasegawa, Okiyama, Takehara, Kohsaka, Fujimoto.

REFERENCES

1. Dalakas MC, Hohlfeld R. Polymyositis and dermatomyositis. Lancet 2003;362:971–82.
2. Engel AG, Arahata K, Emslie-Smith A. Immune effector mechanisms in inflammatory myopathies. Res Publ Assoc Res Nerv Ment Dis 1990;68:141–57.
3. Sugihara T, Sekine C, Nakae T, Kohyama K, Harigai M, Iwakura Y, et al. A new murine model to define the critical pathologic and therapeutic mediators of polymyositis. Arthritis Rheum 2007;56: 1304–14.
4. Gilbert R, Cohen JA, Pardo S, Basu A, Fischman DA. Identification of the A-band localization domain of myosin binding proteins C and H (MyBP-C, MyBP-H) in skeletal muscle. J Cell Sci 1999;112:69–79.
5. Okiyama N, Sugihara T, Iwakura Y, Yokozeki H, Miyasaka N, Kohsaka H. Therapeutic effects of interleukin-6 blockade in a murine model of polymyositis that does not require interleukin-17A. Arthritis Rheum 2009;60:2505–12.
6. Sugihara T, Okiyama N, Suzuki M, Kohyama K, Matsumoto Y, Miyasaka N, et al. Definitive engagement of cytotoxic CD8 T cells in C protein–induced myositis, a murine model of polymyositis. Arthritis Rheum 2010;62:3088–92.
7. Springer TA. Traffic signals for lymphocyte recirculation and leukocyte emigration: the multistep paradigm. Cell 1994;76: 301–14.
8. Ley K, Kansas GS. Selectins in T-cell recruitment to non-lymphoid tissues and sites of inflammation. Nat Rev Immunol 2004;4: 325–35.
9. Luster AD, Alon R, von Andrian UH. Immune cell migration in inflammation: present and future therapeutic targets. Nat Immunol 2005;6:1182–90.
10. Tedder TF, Steeber DA, Pizcueta P. L-selectin deficient mice have impaired leukocyte recruitment into inflammatory sites. J Exp Med 1995;181:2259–64.
11. Grailer JJ, Kodera M, Steeber DA. L-selectin: role in regulating homeostasis and cutaneous inflammation. J Dermatol Sci 2009;56: 141–7.
12. Dustin ML, Rothlein R, Bhan AK, Dinarello CA, Springer TA. Induction by IL 1 and interferon-γ: tissue distribution, biochemistry, and function of a natural adherence molecule (ICAM-1). J Immunol 1986;137:245–53.
13. Steeber DA, Tang ML, Green NE, Zhang XQ, Sloane JE, Tedder TF. Leukocyte entry into sites of inflammation requires overlapping interactions between the L-selectin and intercellular adhesion molecule-1 pathways. J Immunol 1999;163:2176–86.
14. Steeber DA, Campbell MA, Basit A, Ley K, Tedder TF. Optimal selectin-mediated rolling of leukocytes during inflammation in vivo requires intercellular adhesion molecule-1 expression. Proc Natl Acad Sci U S A 1998;95:7562–7.
15. Shimada Y, Hasegawa M, Kaburagi Y, Hamaguchi Y, Komura K, Saito E, et al. L-selectin or ICAM-1 deficiency reduces an immediate-type hypersensitivity response by preventing mast cell recruitment in repeated elicitation of contact hypersensitivity. J Immunol 2003;170:4325–34.
16. Hamaguchi Y, Nishizawa Y, Yasui M, Hasegawa M, Kaburagi Y, Komura K, et al. Intercellular adhesion molecule-1 and L-selectin regulate bleomycin-induced lung fibrosis. Am J Pathol 2002;161: 1607–18.
17. Nagaoka T, Kaburagi Y, Hamaguchi Y, Hasegawa M, Takehara K, Steeber DA, et al. Delayed wound healing in the absence of intercellular adhesion molecule-1 or L-selectin expression. Am J Pathol 2000;157:237–47.
18. Arbones ML, Ord DC, Ley K, Ratech H, Maynard-Curry C, Otten G, et al. Lymphocyte homing and leukocyte rolling and migration are impaired in L-selectin deficient mice. Immunity 1994;1: 247–60.
19. Sligh JE Jr, Ballantyne CM, Rich SS, Hawkins HK, Smith CW, Bradley A, et al. Inflammatory and immune responses are impaired in mice deficient in intercellular adhesion molecule 1. Proc Natl Acad Sci U S A 1993;90:8529–33.
20. Maeda S, Fujimoto M, Matsushita T, Hamaguchi Y, Takehara K, Hasegawa M. Inducible costimulator (ICOS) and ICOS ligand signaling has pivotal roles in skin wound healing via cytokine production. Am J Pathol 2011;179:2360–9.
21. Dernedde J, Rausch A, Weinhart M, Enders S, Tauber R, Licha K, et al. Dendritic polyglycerol sulfates as multivalent inhibitors of inflammation. Proc Natl Acad Sci U S A 2010;107:19679–84.
22. Kaburagi Y, Hasegawa M, Nagaoka T, Shimada Y, Hamaguchi Y, Komura K, et al. The cutaneous reverse Arthus reaction requires intercellular adhesion molecule 1 and L-selectin expression. J Immunol 2002;168:2970–8.
23. Komura K, Hasegawa M, Hamaguchi Y, Saito E, Kaburagi Y, Yanaba K, et al. UV light exposure suppresses contact hypersensitivity by abrogating endothelial intercellular adhesion molecule-1 up-regulation at the elicitation site. J Immunol 2003; 171:2855–62.
24. Matsushita Y, Hasegawa M, Matsushita T, Fujimoto M, Horikawa M, Fujita T, et al. Intercellular adhesion molecule-1 deficiency attenuates the development of skin fibrosis in tight-skin mice. J Immunol 2007;179:698–707.
25. Tang ML, Steeber DA, Zhang XQ, Tedder TF. Intrinsic differences in L-selectin expression levels affect T and B lymphocyte subset-specific recirculation pathways. J Immunol 1998;160: 5113–21.
26. Richards H, Longhi MP, Wright K, Gallimore A, Ager A. CD62L (L-selectin) down-regulation does not affect memory T cell distribution but failure to shed compromises anti-viral immunity. J Immunol 2008;180:198–206.
27. Yang S, Liu F, Wang QJ, Rosenberg SA, Morgan RA. The shedding of CD62L (L-selectin) regulates the acquisition of lytic activity in human tumor reactive T lymphocytes. PLoS One 2011;6:e22560.
28. Okiyama N, Sugihara T, Oida T, Ohata J, Yokozeki H, Miyasaka N, et al. T lymphocytes and muscle condition act like seeds and soil in a murine polymyositis model. Arthritis Rheum 2012;64:3741–9.
29. Kogan TP, Dupre B, Bui H, McAbee KL, Kassir JM, Scott IL, et al. Novel synthetic inhibitors of selectin-mediated cell adhesion: synthesis of 1,6-bis[3-(3-carboxymethylphenyl)-4-(2-α-D-mannopyranosyloxy)phenyl]hexane (TBC1269). J Med Chem 1998; 41:1099–111.
30. Beeh KM, Beier J, Meyer M, Buhl R, Zahlten R, Wolff G. Bimosiamose, an inhaled small-molecule pan-selectin antagonist, attenuates late asthmatic reactions following allergen challenge in

mild asthmatics: a randomized, double-blind, placebo-controlled clinical cross-over-trial. Pulm Pharmacol Ther 2006;19:233–41.
31. Friedrich M, Bock D, Philipp S, Ludwig N, Sabat R, Wolk K, et al. Pan-selectin antagonism improves psoriasis manifestation in mice and man. Arch Dermatol Res 2006;297:345–51.
32. Schlag G, Redl HR, Till GO, Davies J, Martin U, Dumont L. Anti-L-selectin antibody treatment of hemorrhagic-traumatic shock in baboons. Crit Care Med 1999;27:1900–7.
33. Seekamp A, van Griensven M, Dhondt E, Diefenbeck M, Demeyer I, Vundelinckx G, et al. The effect of anti-L-selectin (aselizumab) in multiple traumatized patients–results of a phase II clinical trial. Crit Care Med 2004;32:2021–8.
34. Leonardi C, Menter A, Hamilton T, Caro I, Xing B, Gottlieb AB. Efalizumab: results of a 3-year continuous dosing study for the long-term control of psoriasis. Br J Dermatol 2008;158: 1107–16.

DOI 10.1002/art.38622

Clinical Images: Focal myositis demonstrated on positron emission tomography

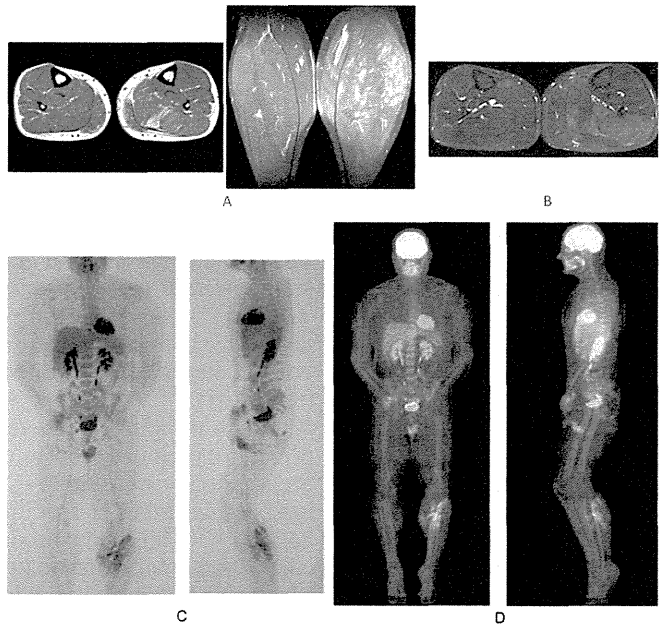

The patient, a 43-year-old man, presented with a 3-month history of pain and swelling involving the posterior part of his left calf, which was exacerbated by palpation. The circumference of the left calf was 3 cm greater than that of the right calf. He denied having any generalized symptoms, including fever, weight loss, or muscle weakness. Laboratory testing revealed elevated levels of creatine phosphokinase (3,470 IU/liter [normal <130 IU/liter]). The results of autoantibody screening tests (rheumatoid factor, antinuclear antibodies, anti–Jo-1, PL-7, PL-12, and anti–signal recognition particle) were negative. The patient had negative findings on serologic tests for infection with cytomegalovirus, Epstein-Barr virus, coxsackievirus, parvovirus, hepatitis virus, human immunodeficiency virus, and *Toxoplasma*. A heterogeneous mass involving the medial head of the left gastrocnemius and soleus muscles was shown on gadolinium-enhanced T1-weighted (**A**) and T2-weighted (**B**) magnetic resonance images. Positron emission tomography (PET) (**C**) and ^{18}F-fluorodeoxyglucose(FDG)–PET scanning (**D**) revealed marked uptake of FDG in the left calf muscles. Histologic assessment of the muscles confirmed the diagnosis of focal myositis, with findings of inflammatory infiltrates associated with necrosis and degeneration/regeneration of muscle fibers. Subsequently, the patient was given prednisone therapy (at an initial dosage of 30 mg/day), which resulted in resolution of the focal myositis. This case supports the notion that FDG-PET scanning is a noninvasive test that is helpful for providing both detailed and complete morphofunctional cartography of muscle changes and guiding muscle biopsy. Thus, when compared with magnetic resonance imaging, FDG-PET scanning has the advantage of showing the absence of other sites of muscle inflammation, which confirms the diagnosis of focal myositis, and excluding underlying malignancy associated with myositis.

Isabelle Marie, MD, PhD
Gaetan Sauvêtre, MD
Stéphanie Becker, MD
Anne-Laure Bedat-Millet, MD
Centre Hospitalier Universitaire Rouen
Rouen, France